UNIVERSITY OF CALIFORNIA SAN DIEGO

Role of Long Non-coding RNAs in Kaposi's Sarcoma-Associated Herpesvirus Lytic Reactivation

A Thesis submitted in partial satisfaction for the degree Master of Science

in

Biology

by

Wanyu Li

Committee in charge:

Professor Tariq Rana, Chair

Professor Amy Pasquinelli, Co-chair

Professor Michael David

The thesis of Wanyu Li is approved, and it is acceptable in quality and form for publication on microfilm and electronically:

_____

_____
Co-chair

_____
Chair

University of California San Diego

2020

TABLE OF CONTENTS

LIST OF FIGURES

LIST OF GRAPHS

LIST OF TABLES

ACKNOWLEDGEMENTS

I would like to acknowledge Dr. Tariq Rana's invaluable support for this project as my thesis advisor and committee chair. Despite my lack of experience as a researcher, Dr. Rana gave me the opportunity to study in his lab and while working on this independent project. His input and encouragement have been essential especially at times when I encountered major obstacles on the project.

I would also like to thank Hui Hui for her immense contribution for the bioinformatics analyses. Though working on multiple projects at once, Hui Hui helped me analyze data from two RNA-seq experiments, and constructed the volcano plots. Her hard work is central to the progress of this project.

Finally, I would like to acknowledge Dr. Qiong, Zhang and Dr. Shaobo, Wang for mentoring me throughout this project. They taught me most of the techniques I used for the project, as well as provided me guidance on the direction of the project, on experimental design, and during troubleshooting. The support I received from everyone who has been with me since I entered the Rana Lab is integral not only to this project, but also to my education as a scientific researcher.

ABSTRACT OF THE THESIS

Role of Long Non-coding RNAs in Kaposi's Sarcoma-Associated Herpesvirus Lytic Reactivation

by

Wanyu Li

Master of Science in Biology

University of California San Diego, 2020

Professor Tariq Rana, Chair

Professor Amy Pasquinelli, Co-chair

Professor Michael David

Kaposi's sarcoma-associated herpesvirus (KSHV) is the etiological agent of Kaposi's sarcoma, an AIDS-related endothelial malignancy. In an infected cell population, KSHV largely exists as a latent episome, while a small percentage of latent virus undergoes lytic reactivation. The latent-to-lytic switch of KSHV is pathologically important, tightly regulated event that involves extensive host-virus crosstalk. Long non-coding RNAs (lncRNAs) are a diverse class of RNA regulators that have been shown to involve in the life cycles of many different viruses. However, the roles of lncRNAs in KSHV lytic reactivation have been unexplored. This study utilizes two cellular models of KSHV latent infection of different tissue origins to uncover differentially expressed lncRNAs during KSHV lytic reactivation via RNA-seq, revealing lncRNAs that may function in modulating virus lytic replication. Using CRISPR interference (CRISPRi), one of the novel differentially expressed lncRNAs, AC017002.3, was found to positively regulate KSHV early lytic transcript level. Since lncRNAs tend to function in ribonucleoprotein complexes, to address the mechanism by which AC017002.3 functions, RNA affinity pull-down was performed to search for its potential interacting proteins. hnRNP K and ILF2 were found to associate with AC017002.3. While functional validation of possible ribonucleoproteins involving AC017002.3 need to be conducted, this study provides the first evidence that host lncRNAs regulate KSHV lytic reactivation.

Chapter 1: Introduction

1.1 KSHV

Kaposi's sarcoma-associated herpesvirus (KSHV), formerly known as human gammaherpesvirus 8 (HHV-8), is a large double-stranded DNA (dsDNA) virus belonging to the *Herpesviridae* family. It is the etiological agent of Kaposi's sarcoma (KS), a malignancy found in immunocompromised individuals, particularly AIDS patients (Mesri et al., 2010). KSHV infection has also been associated with B cell lymphoproliferative diseases, including primary effusion lymphoma (PEL) and specific forms of multicentric Castleman disease (MCD) (Goncalves et al., 2017; Karcher and Alkan, 1995). KSHV infection is often insufficient to give rise to KS without additional external factors, such as HIV co-infection (Mesri et al., 2010).

The seroprevalence of KSHV has been estimated to be low in the Americas and Europe and higher in certain Mediterrancean countries and Africa (Schulz, 2000). It is endemic in sub-Saharan Africa, where seroprevalence was estimated to reach 40% (Chatlynne and Ablashi, 1999). Transmission of KSHV could be achieved through unprotected sex, saliva, organ transplantation, and blood transfusion (He et al., 1998; Kedes et al., 1996; Mesri et al., 2010). Treatment options include common anti-herpesvirus drugs such as ganciclovir, foscarnet, and cidofovir, chemotherapy, and radiotherapy (Coen et al., 2014). For treatment of AIDS-related KS, highly active antiretroviral therapy (HAART) can be effective (Yarchoan et al., 2005). At presence, KSHV poses important public health threat in certain geographic regions, inasmuch as treatment strategies for KS are not curative and vaccines are unavailable (Mesri et al., 2010). Studying the molecular virology of KSHV facilitates understanding of key regulatory pathways involved in its life cycle, thereby helps identify potential therapeutic targets.

1.1.1 KSHV Latency and Lytic Reactivation

In both KS spindle cells and PEL cells, KSHV manifests two distinct stages of infection. In lytic infection, structural genes are expressed, accompanied by active virion production and cell lysis, but in latent infection, only a small set of latency-associated genes are expressed, without productive virion

production (Mesri et al., 2010). A small portion of latent virus in KS and PEL could show spontaneous lytic reactivation, and this has been speculated to be important for maintaining the population of infected cells against the loss of latent viral genomes from cell death and with cell passage (Aneja and Yuan, 2017; Sun et al., 1999). In latently infected cells, the KSHV genome is a histone-associated episome, where suppressive chromatin modification prevents lytic genes from effective expression and only a concentrated region encoding latency-associated nuclear antigen (LANA), vCyclin, vFLIP, and viral

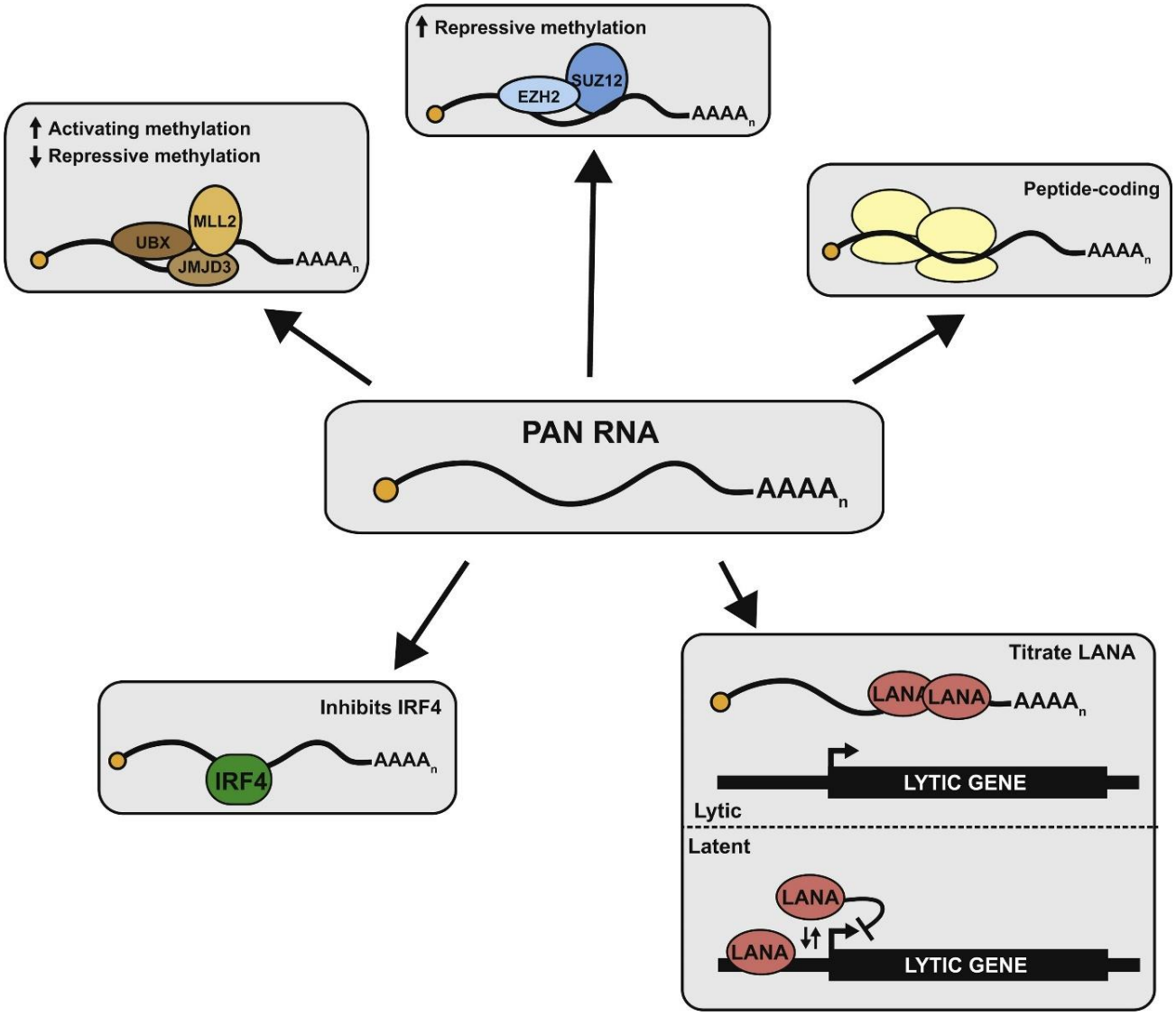

Figure 1.1.1: Proposed PAN RNA functions (Conrad, 2016).

microRNAs (miRNAs) undergoes active transcription (Mesri et al., 2010; Toth et al., 2013). The latent-to-lytic switch is accomplished by the viral replication and transcription activator (RTA) protein, expressed from the *ORF50* gene, which can stimulate viral promoters containing an RTA response element (RRE), as well as the *ORF50* promoter itself (Deng et al., 2000; Gradoville et al., 2000). Essential early lytic genes include *PAN* and *K8*. PAN is a KSHV-encoded lncRNA of approximately 1kb in length, and its transcript level can be upregulated to extreme abundance, averaging over 10^5 copies per cell, accounting for the majority of cellular polyadenylated RNAs (Conrad, 2016; Zhong et al., 1996). PAN is multifunctional, playing roles in repressing the major latency maintainer LANA, altering histone modification, antagonizing innate immunity, and even coding for small peptides from small open reading frames (sORFs) (Figure 1.1.1) (Conrad, 2016). PAN mutants are not able to be productively reactivated even with fully functional RTA (Rossetto and Pari, 2012). K8 is a multifunctional protein that can recruit DNA replication machineries to the origin of lytic DNA replication, or repress global RTA-dependent transcriptional activation (Liao et al., 2003; Wang et al., 2008). Both *PAN* and *K8* can be transactivated by RTA, through an RRE in the promoter in the case of *PAN*, and through a seemingly RRE-independent mechanism in the case of *K8* (Lukac et al., 2001; Song et al., 2002; Wang et al., 2003a). PAN has been shown to broadly bind the KSHV episome including *K8*, and the expression of K8 among most lytic proteins was downregulated in the reactivation of PAN-deleted mutant virus compared to wild-type, suggesting a role for PAN in the regulation of lytic transcript levels (Rossetto et al., 2013).

Both the lytic and the latent phases contribute to KSHV pathogenesis, and lying at the regulatory center of them is the reactivation event. The lytic phase is not thought to be directly tumorigenic, because infected cells are killed and host genes are subject to global shutoff (Glaunsinger and Ganem, 2004). Latently infected cells, on the other hand, retain host transcriptional activity and, at the same time, produce oncogenic viral latent proteins: LANA has been shown to suppress p53, kaposin B has been shown to promote chronic inflammation, and vFLIP has been shown to activate NFκB and prohibit apoptosis (Guasparri et al., 2004; King, 2013; Si and Robertson, 2006). Lytic genes, such as vGPCR, K1, and vIL-6, also have oncogenic potentials, as they stimulate intercellular growth factor signaling and

angiogenesis, suppress apoptosis, and promote inflammation (Jham et al., 2011; Sakakibara and Tosato, 2011; Tomlinson and Damania, 2004). An integrative model proposes that constitutive lytic reactivation in KSHV-infected tissues maintains the latent viral pool and promotes a tumor-friendly microenvironment, in which reactivated cells produce progeny virions that invade uninfected cells, at the same time releasing growth factors, pro-inflammatory cytokines and boosting angiogenesis to allow latently infected cells to undergo cancerous growth (Mesri et al., 2010). Lytic reactivation is therefore

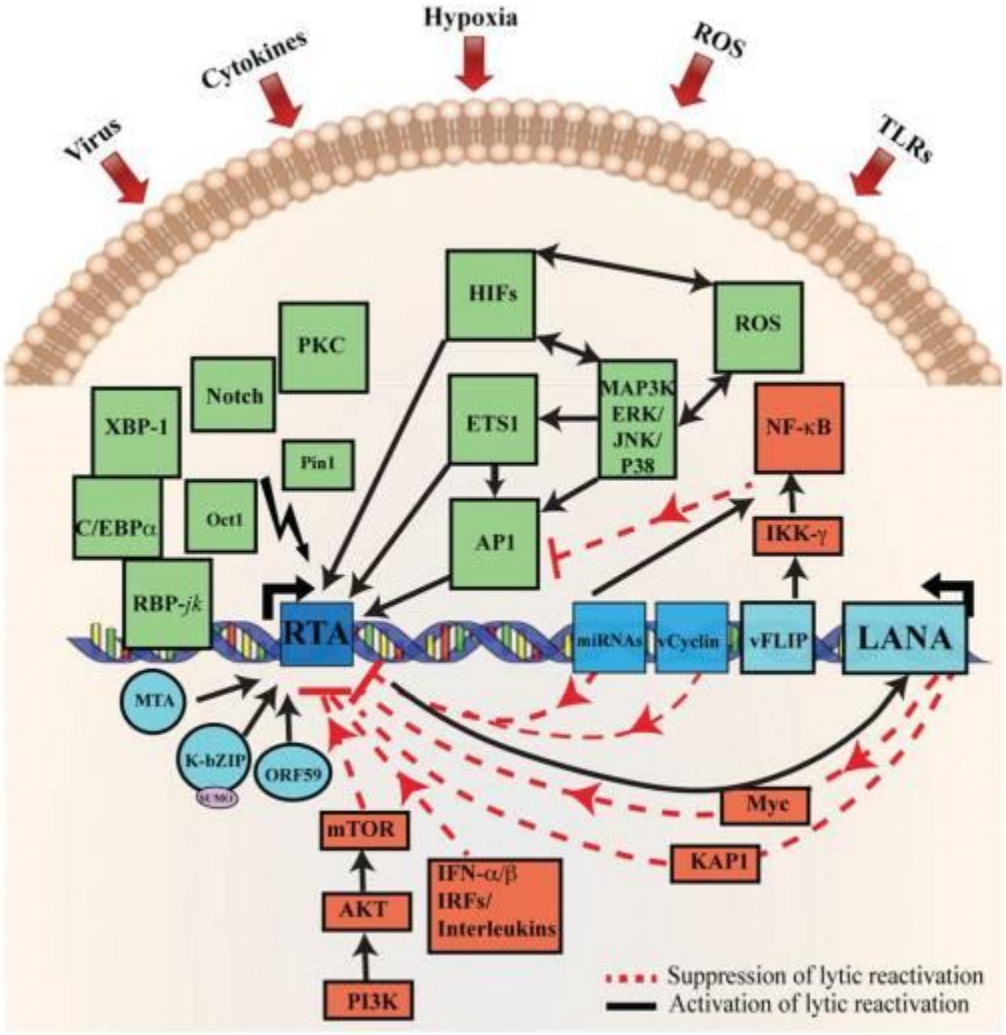

Figure 1.1.2: Cellular factors and external stimuli shown to regulate KSHV lytic reactivation (Purushothaman et al., 2015).

very likely pathologically relevant and understanding the molecular regulation of this event facilitates therapeutic development. To this end, many hosts proteins have been found to function in this intricately regulated event (Figure 1.1.2) (Davis et al., 2015; Grossmann and Ganem, 2008; Tan et al., 2018; Toth et al., 2013; Wang et al., 2003b; Zhang et al., 2020).

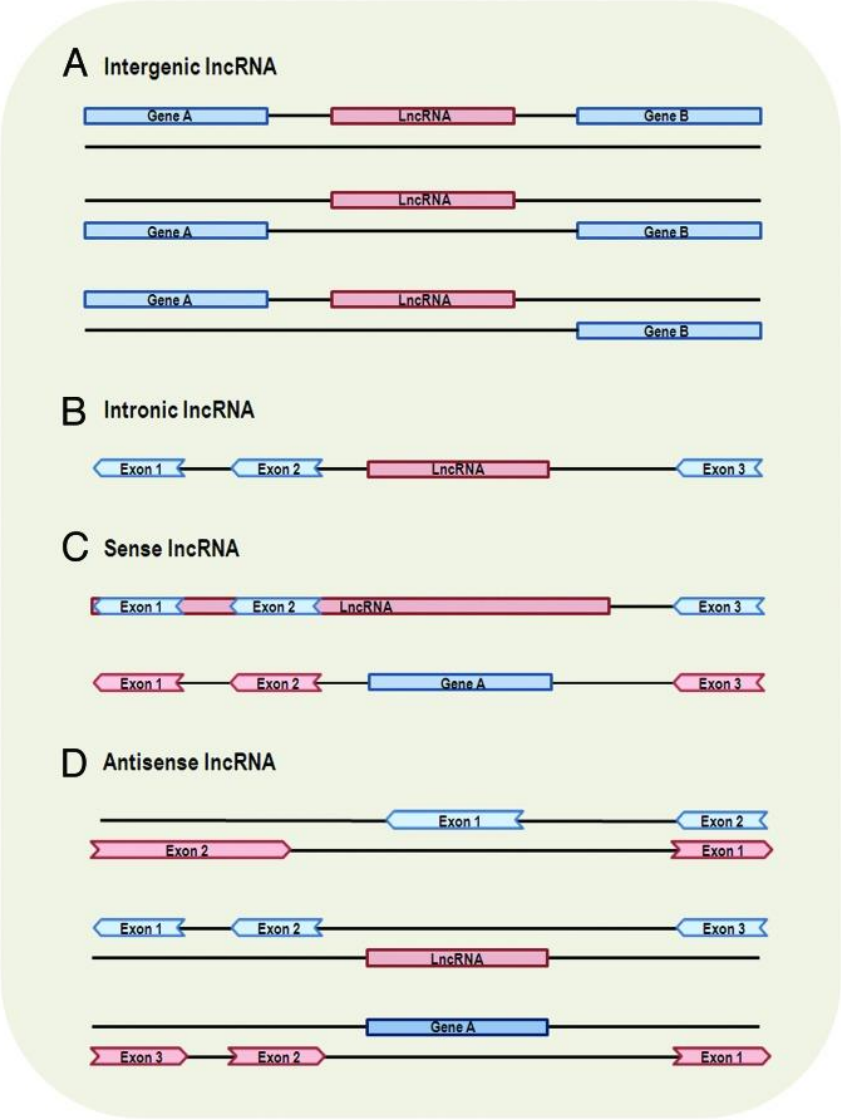

Figure 1.2.1: Common genomic locations of lncRNAs (Ma et al., 2013).

1.2 LncRNAs

Long non-coding RNAs (lncRNAs) refer to non-coding transcripts more than 200 nucleotides in length. Potentially taking up a significant share of the human genome, they comprise a class of still

relatively underexplored cellular regulatory module (Fortes and Morris, 2016). Similar to mRNAs, lncRNAs are transcribed by RNA polymerase II (pol II), capped at the 5 prime and polyadenylated at the 3 prime (Guttman et al., 2009; Ulitsky and Bartel, 2013). Their expression tends to be lower than that of mRNAs, and more tissue-specific (Clark et al., 2011; Derrien et al., 2012). LncRNAs could be found in intergenic regions, within introns of coding genes, sense or antisense to coding genes, and they have been classified accordingly, but functional classification will require better understanding of these RNAs grouped under the catch-all "long non-coding RNA" (Figure 1.2.1) (Ma et al., 2013; Ulitsky and Bartel, 2013).

LncRNAs function through diverse mechanisms, many involving complexing in ribonucleoprotein complexes but there are solely RNA-mediated mechanisms as well (Ma et al., 2013). Ribonucleoprotein complexes may involve lncRNAs with chromatin modification factors, transcription elongation complex components, splicing factors, translation factors and more, where they regulate the pathways

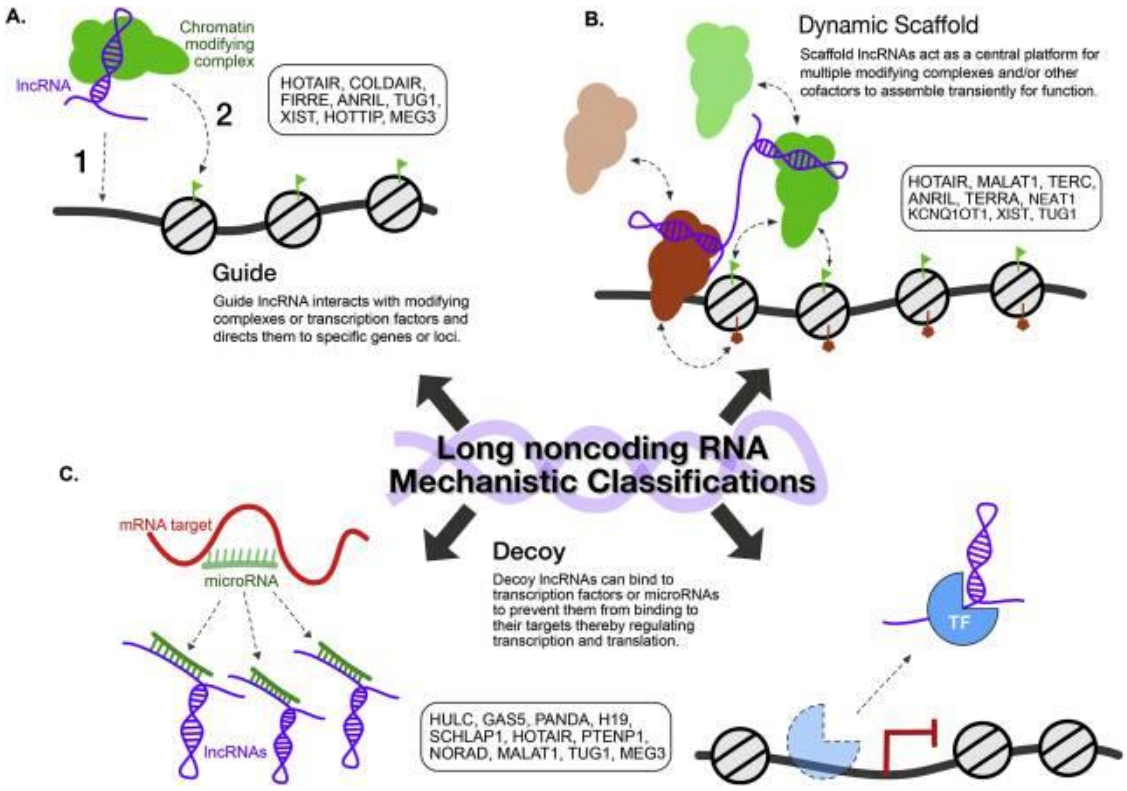

Figure 1.2.2: Examples of lncRNA mechanisms employed by known lncRNAs (Balas and Johnson, 2018).

corresponding to the relevant ribonucleoprotein complexes (Li et al., 2014; Lin et al., 2008; Nguyen et al., 2001; Tripathi et al., 2010; Zhang et al., 2019). For transcriptional control, lncRNA could bind genomic DNA and recruit transcription factors to exert regulation (Figure 1.2.2) (Zhang et al., 2019). Alternatively, lncRNAs may also directly bind RNA. lncRNAs binding to mRNA may affect mRNA stability through subjecting target mRNAs to decay pathways, while lncRNAs containing microRNA (miRNA) target sites may serve as "sponges" for mRNAs that are targeted by those miRNAs (Figure 1.2.2) (Cesana et al., 2011; Gong and Maquat, 2011). In some cases, the transcription event of the lncRNAs could itself exert transcriptional interference by letting pol II travel through an overlapping segment of regulatory DNA element (Latos et al., 2012). As more lncRNAs are characterized, understanding of RNA-dependent mechanisms will continuously expand.

1.2.1 LncRNA Functions in Viral Life Cycle

Many host lncRNAs have been shown to regulate virus infection and replication. Some are dependence factors for the viral life cycle, and are differentially regulated by viruses. The lncRNA HEAL is recruited by HIV-1 to its promoter to boost transcription, and is upregulated by HIV infection (Chao et al., 2019). The lncRNA PCNAP1 sponges miR-154 and thereby upregulates PCNA, which binds hepatitis B virus (HBV) cccDNA and enhances HBV replication (Feng et al., 2019). PCNAP1 is also upregulated by HBV infection (Feng et al., 2019). An interferon-stimulated lncRNA, lnc-Lsm3b, sequesters the innate RNA sensor RIG-I in its inactive form, thereby regulating immune homeostasis but restricts innate immune response to viral infection (Figure 1.2.3) (Jiang et al., 2018). Other lncRNAs function as restriction factors. LncRNA#32 is complexed with hnRNP U and ATF2 and positively regulates interferon-stimulated gene (ISG) expression to confer resistance to encephalomyocarditis virus (EMCV) (Nishitsuji et al., 2016). LncITPRIP-1 is a lncRNA inducible by viral infection and promotes the RNA sensor MDA5 function, consequently enhancing innate immune response to hepatitis C virus (HCV) infection (Xie et al., 2018). Lnc-ISG20, an interferon-stimulated lncRNA, sponges miR-326, thereby upregulating the miR-326 target ISG20 mRNA and promoting innate immune response that suppresses

influenza A virus (IAV) (Chai et al., 2018). Not only do host lncRNAs regulate viral life cycles, the reverse is also true, as host cell lncRNA landscape is globally and systemically altered in response to activity of the viral life cycle, suggesting functionally important host-virus crosstalk (Chao et al., 2019; Hu et al., 2016; Peng et al., 2010; Zhang et al., 2016).

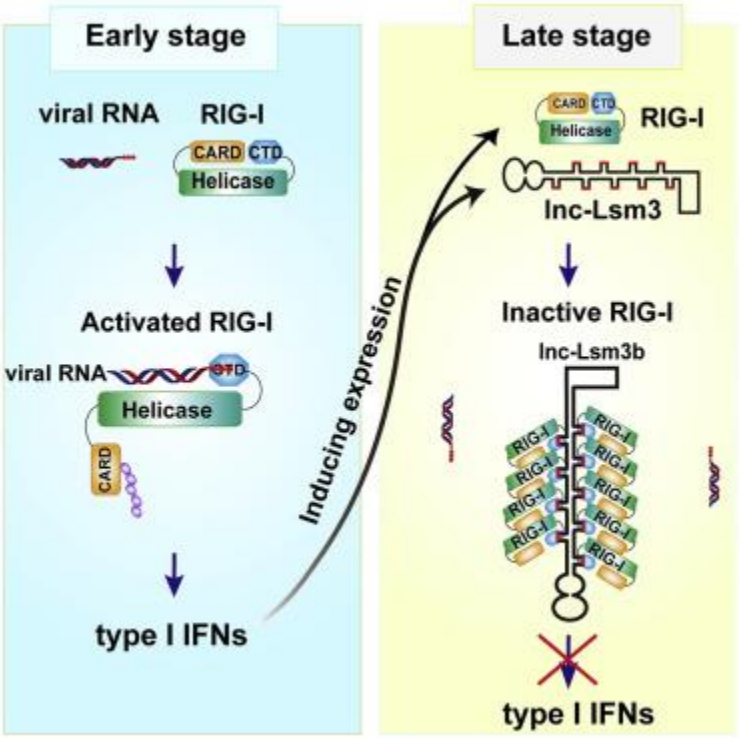

Figure 1.2.3: Mechanism of function by lnc-Lsm3b (Jiang et al., 2018).

1.3 Aims of the Study

Whether and how host lncRNAs participate in KSHV lytic reactivation is unknown. Given the global differential regulation of lncRNA expression in response to viral infection, and the documented lncRNA modulation of viral activity, it is likely that KSHV lytic reactivation also induces extensive change in the host lncRNA landscape, which in turn regulates the reactivation program. This study aims to uncover differentially expressed lncRNAs during KSHV lytic reactivation, and to functionally characterize novel lncRNAs in the context of lytic gene expression.

- Illustrate the long non-coding transcriptome during KSHV lytic reactivation
- Characterize the differentially expressed novel lncRNA AC017002.3
- Study the regulation of KSHV lytic gene expression by AC017002.3
- Examine potential ribonucleoprotein complexed that involve AC017002.3

Chapter 2: Results

2.1 LncRNA Landscape in KSHV Reactivation

2.1.1 Cellular Models of KSHV Infection

To study the lncRNA landscape during KSHV lytic reactivation, two cellular models of KSHV latent infection were utilized. iSLK cells are of epithelial origin, harboring latent KSHV episomes that expresses a puromycin resistant gene and GFP (Myoung and Ganem, 2011; Sturzl et al., 2013). These cells also carry a hygromycin selectable cassette of RTA expression under a promoter containing a tetracycline response element (TRE), which can be activated by a reverse tetracycline controlled transactivator (rtTA) that presents the herpes simplex virus 1 VP16 transcriptional activation domain (Figure 2.1.1) (Gossen et al., 1995; Myoung and Ganem, 2011). rtTA is constitutively expressed by a third exogenous construct, and when doxycycline is present, uses doxycycline as a co-factor to drive RTA expression, which in turn leads to broad lytic gene activation and lytic-to-latent switching (Figure 2.1.1) (Myoung and Ganem, 2011). Dose-dependent expression of KSHV lytic genes could be observed when doxycycline was added to iSLK cells, where the early transcript PAN is induced to extremely high levels (Graph 2.1.1).

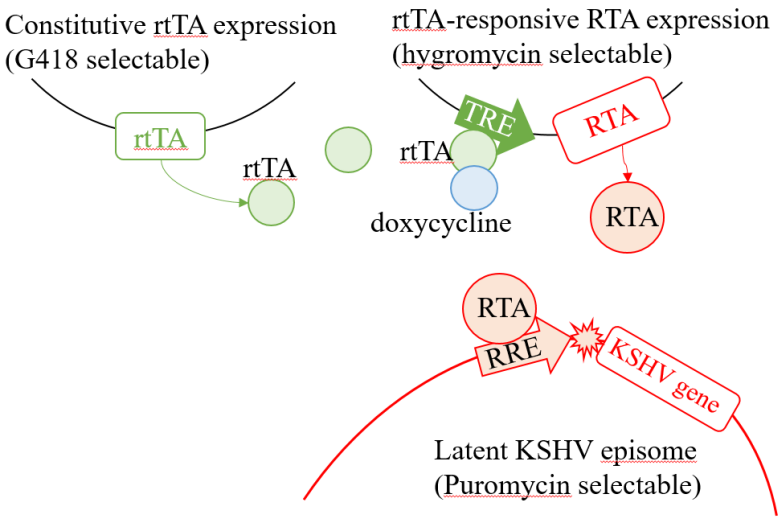

Figure 2.1.1: iSLK model of KSHV infection. iSLK cells constitutively expresses rtTA, which requires doxycycline as a co-factor to activate the TRE-harboring promoters upstream of RTA. RTA proteins recognizes the RTA response element (RRE) in KSHV endogenous promoters and broadly activates lytic gene expression. rtTA cassette expresses a G418 resistance gene, recombinant RTA cassette expresses a hygromycin resistance gene, and KSHV genome expresses a puromycin resistance gene.

Graph 2.1.1: Doxycycline induces KSHV lytic replication in iSLK cells. iSLK cells were mock- or doxycycline-induced for 48 h, total RNA was extracted, and KSHV lytic gene expression was quantified by qPCR. Bar represents mean ± SD. ***p*<0.01, ****p*<0.001, *****p*<0.0001, by Student's *t* test. N = 4.

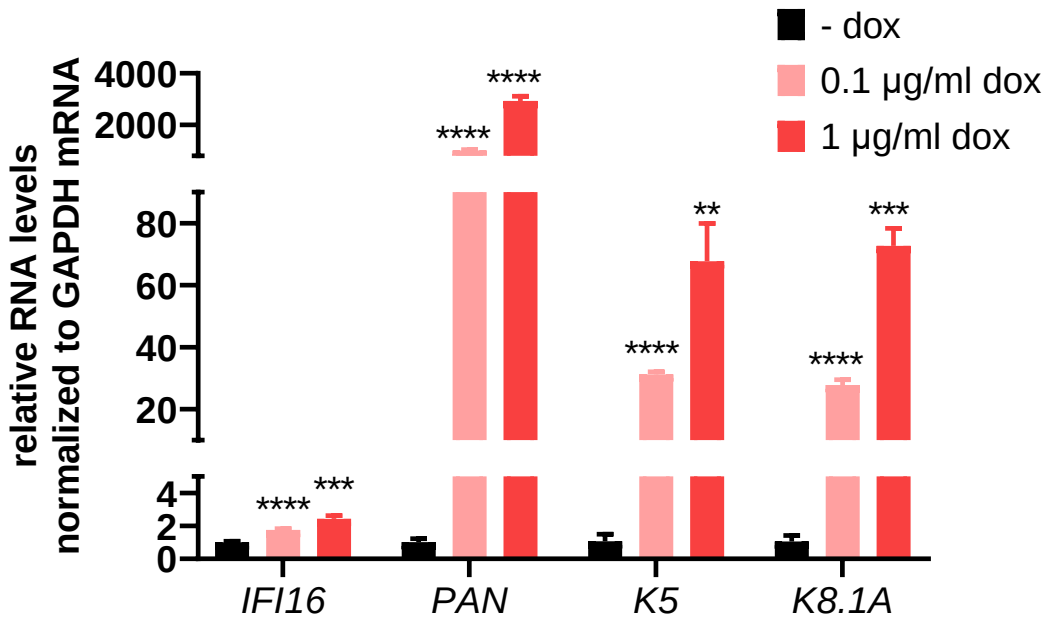

The other model selected for this study, BC-3-G, is a modified PEL cell line. It is generated from BC-3 cells, which are already latently infected by KSHV, by transfecting a GFP expression cassette under a PAN promoter (Figure 2.1.2) (Yu et al., 2007). The small molecular used to induce BC-3-G is terephthalic acid (TPA), which could lead to lytic gene expression including RTA, and RTA in turn stimulates GFP expression (Figure 2.1.2). When BC-3-G cells were treated with this chemical, percentages of GFP+ individuals in the population drastically increased, accompanied by elevated expression of KSHV lytic genes (Graph 2.1.2). To be noted is that without TPA treatment, there was still a considerable percentage of GFP+ cells, indicating high spontaneous reactivation (Graph 2.1.2 A).

In using both iSLK and BC-3-G to uncover the long non-coding transcriptomes during KSHV lytic reactivation, common differentially regulated lncRNAs from both cell types could be revealed. Since lncRNAs tend to have low, tissue- and cell type-specific expression, lncRNAs that are differentially expressed in the same direction in both the epithelial iSLK cells and lymphocytic BC-3-G cells might be

functionally important not only for the KSHV life cycle, but also for fundamental aspects of human cell biology (Clark et al., 2011; Derrien et al., 2012).

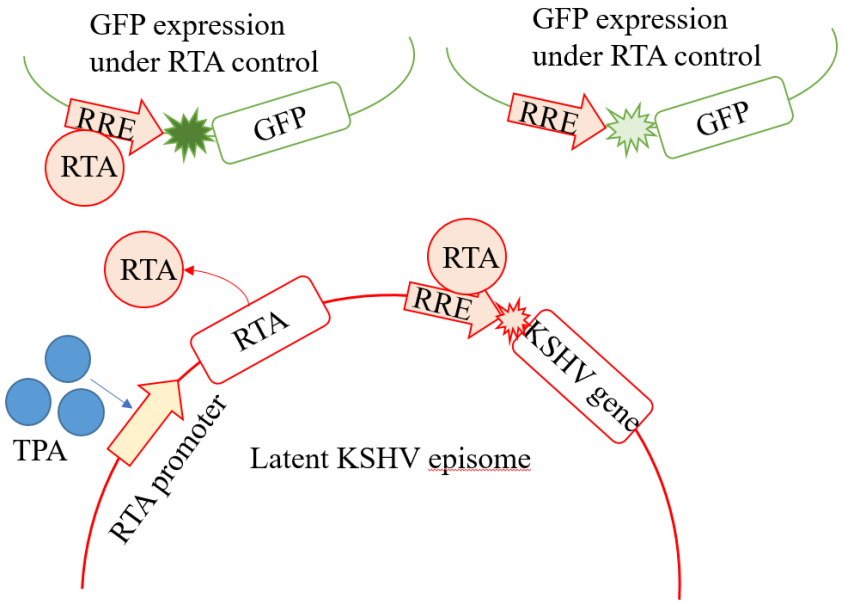

Figure 2.1.2: BC-3-G model of KSHV infection. BC-3-G cells harbor KSHV episomes. TPA activates the promoter of viral endogenous RTA, which drives lytic gene expression and GFP expression from a cassette with RRE. There is constitutively a small fraction of GFP+ cells in the BC-3-G culture, indicating spontaneous reactivation and leaking RTA expression.

Although both cell lines were used in transcriptomic analyses, functional study was primarily conducted on iSLK cells, because they present three main advantages over PEL cell lines. First, reactivation is more tightly controlled in iSLK. Using a Tet-On system to control exogenous RTA expression greatly reduces spontaneous reactivation, which is extensive in PEL cell lines and produces a high background (Myoung and Ganem, 2011). The Kozak sequence, central to efficient translation, is removed from the RTA gene to further suppress leakage (Myoung and Ganem, 2011). High spontaneous reactivation blurs the latent-to-lytic switch in PEL cell lines, making it relatively difficult to manually switch the two phases of the KSHV life cycle in a clear-cut way. Second, TPA is a pleiotropic chemical that dramatically alters cellular pathways, generating the concern that transcriptomic changes in TPA-induced PEL cells are more likely results of nonspecific effects of TPA itself (Myoung and Ganem,

2011). Third, reactivation in iSLK cells proceeds slowly, making it possible to resolve detailed biological timeline and detect nuanced molecular functions (Park et al., 2019; Pringle et al., 2019).

Graph 2.1.2: TPA induces KSHV lytic replication in BC-3-G cells. (A) BC-3-G cells were mock- or TPA-induced for 48 h and subject to flow cytometry analysis. Left panel shows average percentages of GFP+ cells under the treatment of indicated concentrations of TPA. Right panel shows representative flow cytometry plots for each concentration of TPA. N = 3 for left panel. (B) BC-3-G cells were mock- or TPA-induced for 48 h, total RNA was extracted, and KSHV lytic gene expression was quantified by qPCR. Bar represents mean ± SD. *p<0.05, **p<0.01, ***p<0.001, ****p<0.0001, by Student's t test. N = 3.

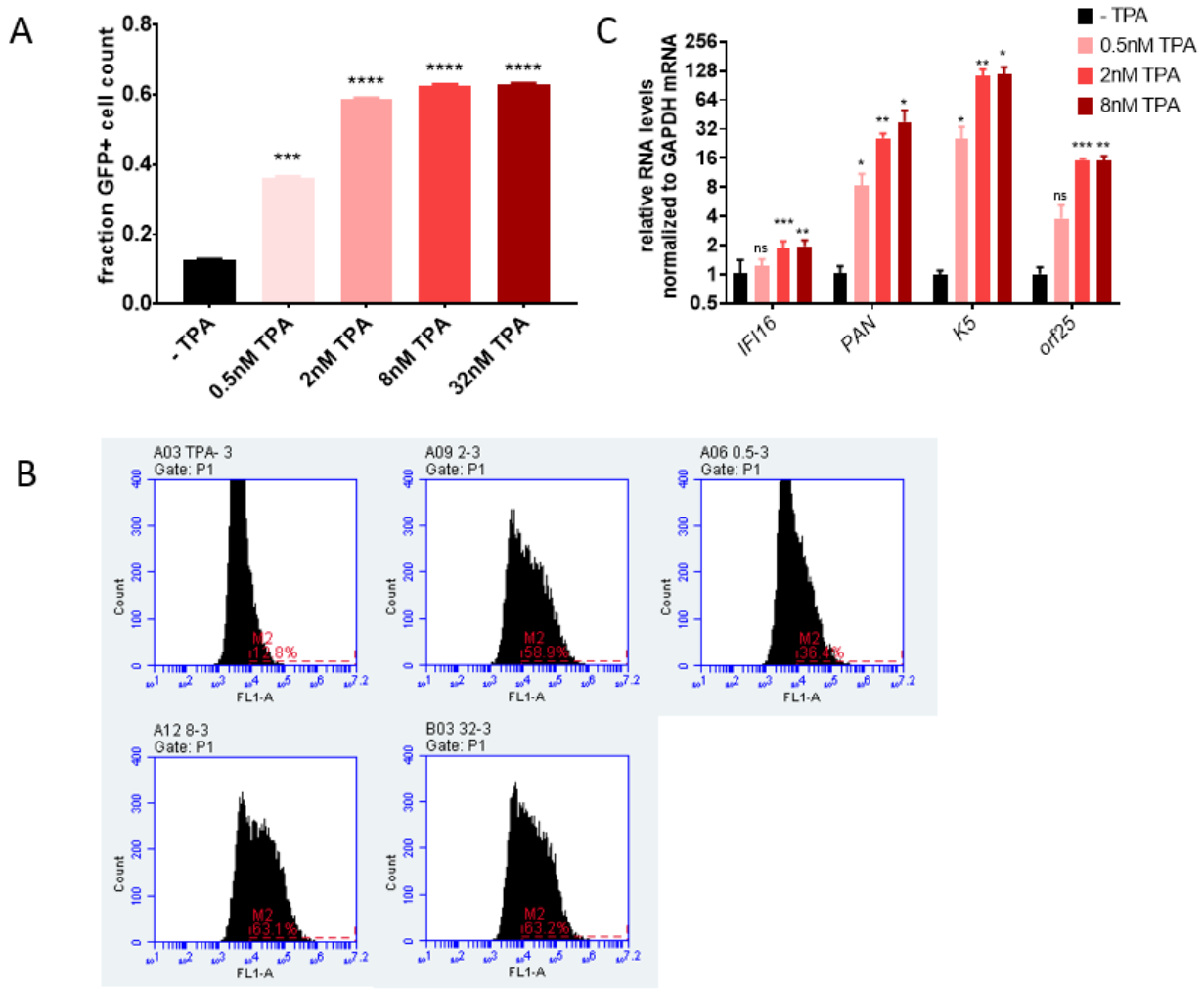

2.1.2 Identification of Differentially Regulated LncRNAs during KSHV Reactivation

Graph 2.1.3 LncRNAs are differentially expressed upon KSHV lytic reactivation in iSLK and BC-3-G cells. (A) iSLK cells were mock- or doxycycline-induced for 48 h, total RNA was extracted and subject to RNA-seq. (B) BC-3-G cells were mock- or TPA-induced for 48 h, total RNA was extracted and subject to RNA-seq. The target selected for further study, AC017002.3 (ENSG00000240350.2), is highlighted. (C) Upregulated and downregulated lncRNAs in induced iSLK and BC-3-G cells were compared, and the numbers of common differentially expressed lncRNAs were summarized. (D) Common upregulated and downregulated lncRNAs in induced iSLK and BC-3-G cells were listed with their $\log_2$ fold change shown in the heatmap. (E) iSLK cells were mock- or doxycycline-induced for 48 h, total RNA was extracted, and the levels of common upregulated and downregulated lncRNAs from (D) were quantified by qPCR. Bar represents mean ± SD. *p<0.05, **p<0.01, ***p<0.001, ****p<0.0001, by Student's t test. N = 4.

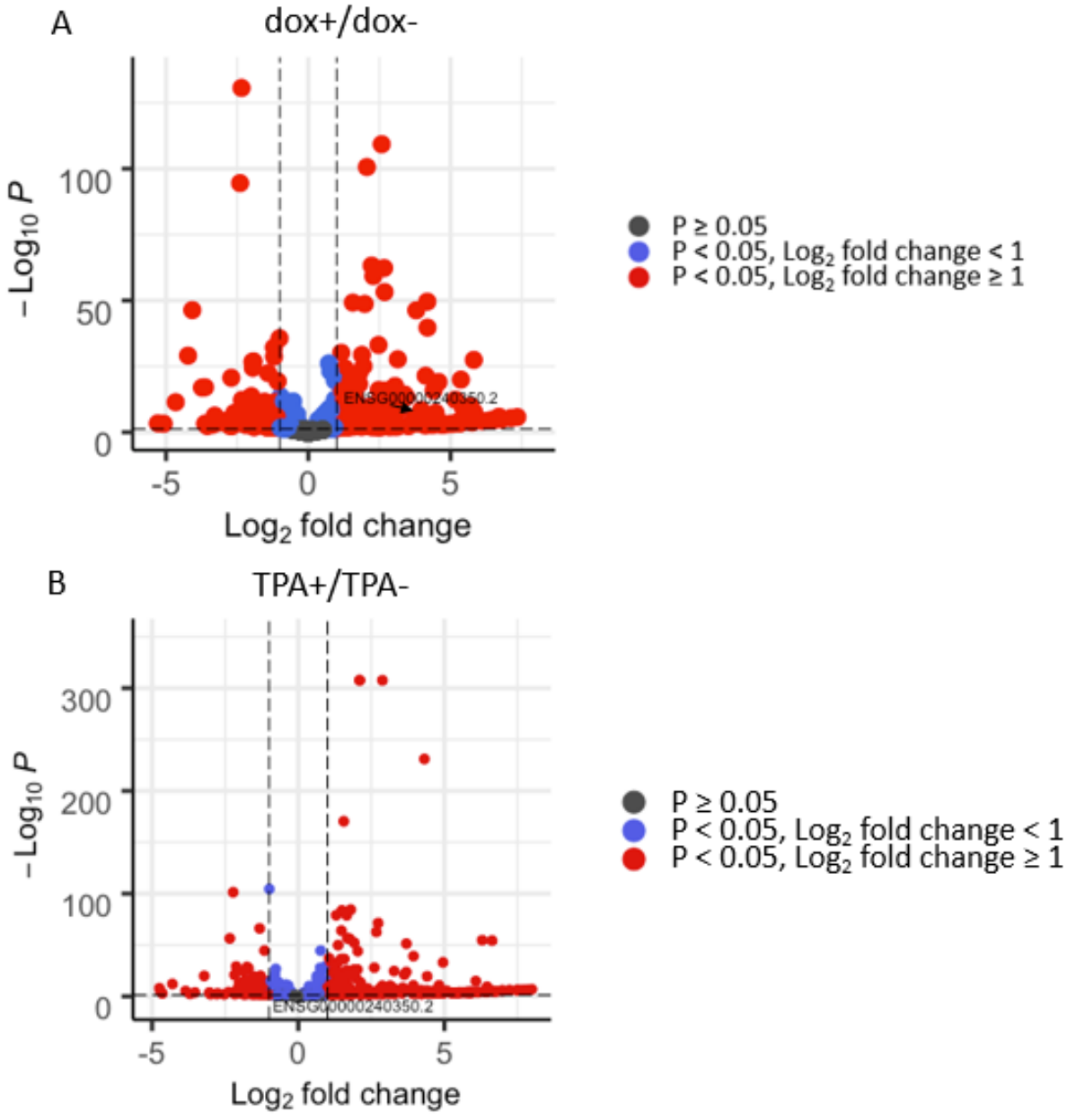

Graph 2.1.3 LncRNAs are differentially expressed upon KSHV lytic reactivation in iSLK and BC-3-G cells. (A) iSLK cells were mock- or doxycycline-induced for 48 h, total RNA was extracted and subject to RNA-seq. (B) BC-3-G cells were mock- or TPA-induced for 48 h, total RNA was extracted and subject to RNA-seq. The target selected for further study, AC017002.3 (ENSG00000240350.2), is highlighted. (C) Upregulated and downregulated lncRNAs in induced iSLK and BC-3-G cells were compared, and the numbers of common differentially expressed lncRNAs were summarized. (D) Common upregulated and downregulated lncRNAs in induced iSLK and BC-3-G cells were listed with their $\log_2$ fold change shown in the heatmap. (E) iSLK cells were mock- or doxycycline-induced for 48 h, total RNA was extracted, and the levels of common upregulated and downregulated lncRNAs from (D) were quantified by qPCR. Bar represents mean ± SD. *p<0.05, **p<0.01, ***p<0.001, ****p<0.0001, by Student's t test. N = 4, Conituned

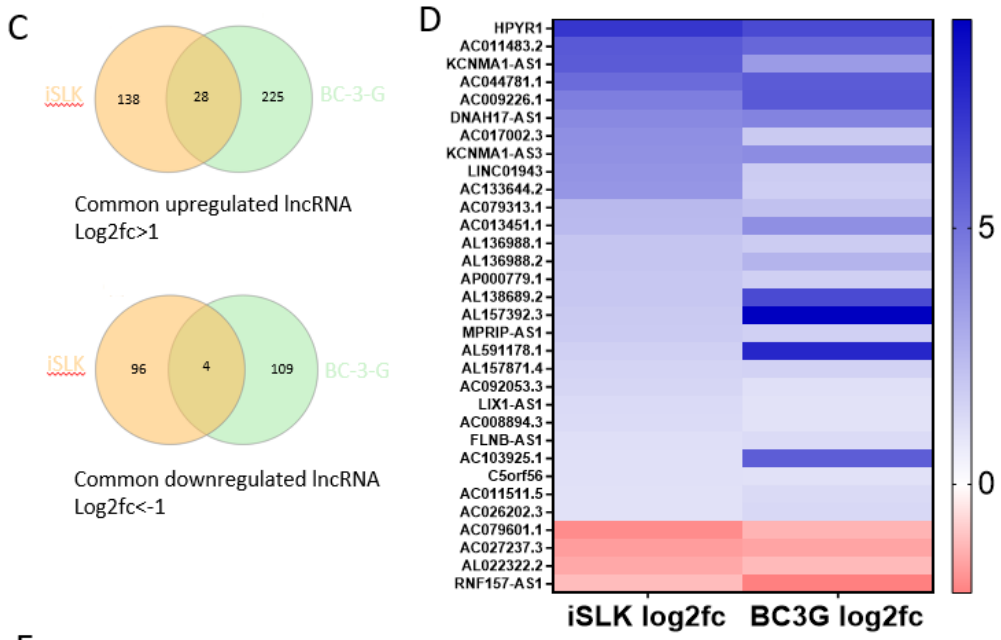

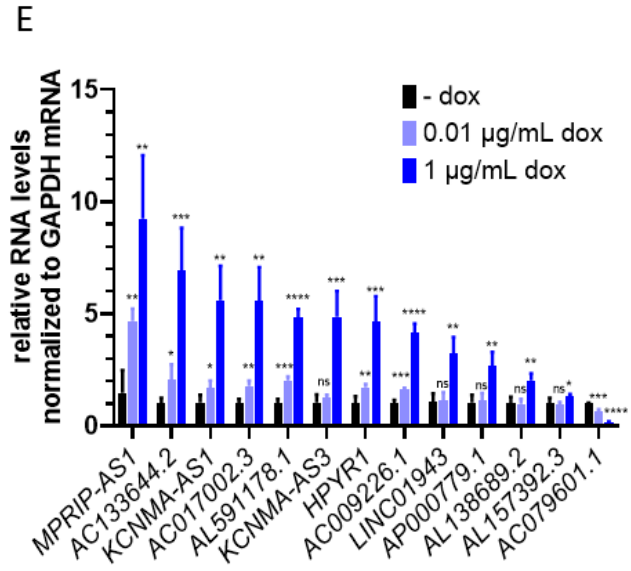

To map out the landscape of lncRNA expression during KSHV reactivation, cDNA library was prepared from total RNA isolated from doxycycline-induced iSLK cells and TPA-induced BC-3-G cells.

Significantly differentially expressed lncRNA genes (log_2 fold change ≥ 1, $p < 0.05$) were identified in both induced iSLK and induced BC-3-G compared to mock controls (Graph 2.1.3 A and B). There were 166 upregulated and 100 downregulated lncRNAs in induced iSLK, 253 upregulated and 113 downregulated lncRNAs in induced in BC-3-G (Graph 2.1.3 C). iSLK and BC-3-G share 28 common upregulated lncRNAs and 4 common downregulated lncRNAs, most of which are antisense to coding genes with a few being intergenic (Graph 2.1.3 C and D). To verify top hits in iSLK cells, which were used for subsequent functional study, total cDNA of doxycycline-induced iSLK cells was subject to qPCR to quantify the expression of target lncRNAs, and targets that return positive were shown in Graph 2.1.3 E. These data present the long non-coding transcriptomes in two KSHV latent cellular models of different tissue origins, uncovering lncRNAs that may be functionally important both in KSHV lytic-to-latent switch and in human cell biology.

2.2 Characterization of AC017002.3

2.2.1 Molecular Characterization of AC017002.3

The full-length sequence of lncRNAs are necessary for functional and mechanistic study, but only error-prone predicted sequences are available for novel lncRNAs. To authenticate full-length sequences of novel lncRNAs, 6 commonly upregulated lncRNAs that exhibit the highest fold change in iSLK cells per qPCR verification were subject to rapid amplification of cDNA ends (RACE). Most novel lncRNAs appear to have multiple isoforms per RACE PCR, complicating functional analysis, since different isoforms could have different functions and are difficult to distinguish by available knock-down or knock-out tools, but AC017002.3, with no isoform, was successfully authenticated (Figure 2.2.1.1 A). To RACE authenticate AC017002.3, two pairs of nested gene specific primers (GSP) were designed to ensure template specificity (Table 2.2.1.1). AC017002.3 is located on the long arm of chromosome 2, with no protein coding genes in sufficient proximity to form a *cis* coding-non-coding gene pair (Figure 2.2.1.1 A). Alignment with predicted AC017002.3 sequence on *Ensembl.org* shows that the authenticated transcript differs at both ends, and is overall shorter (Figure 2.2.1.1 B).

Some lncRNAs have coding potential, producing functional small peptides that partake in cellular pathways (Choi et al., 2019; Rion and Ruegg, 2017). To check whether potential functions exerted by AC017002.3 would be due to the RNA itself or small peptides, the coding potential of AC017002.3 was examined. AC017002.3 was cloned into pFLAG-CMV in the sense or antisense directions, or in the sense direction

Table 2.2.1.1: Primers used in RACE PCR of AC017002.3.

	Primer sequence
3'GSP	CTTCCCTGATAATCAAGCC
5'GSP	CAGGGCTTTGTGTGTAATC
3'NGSP	AATAATTCTTCCTAGAACAACTCC
5'NGSP	AAGCCAGCTAGAGTAAATTTCTAG

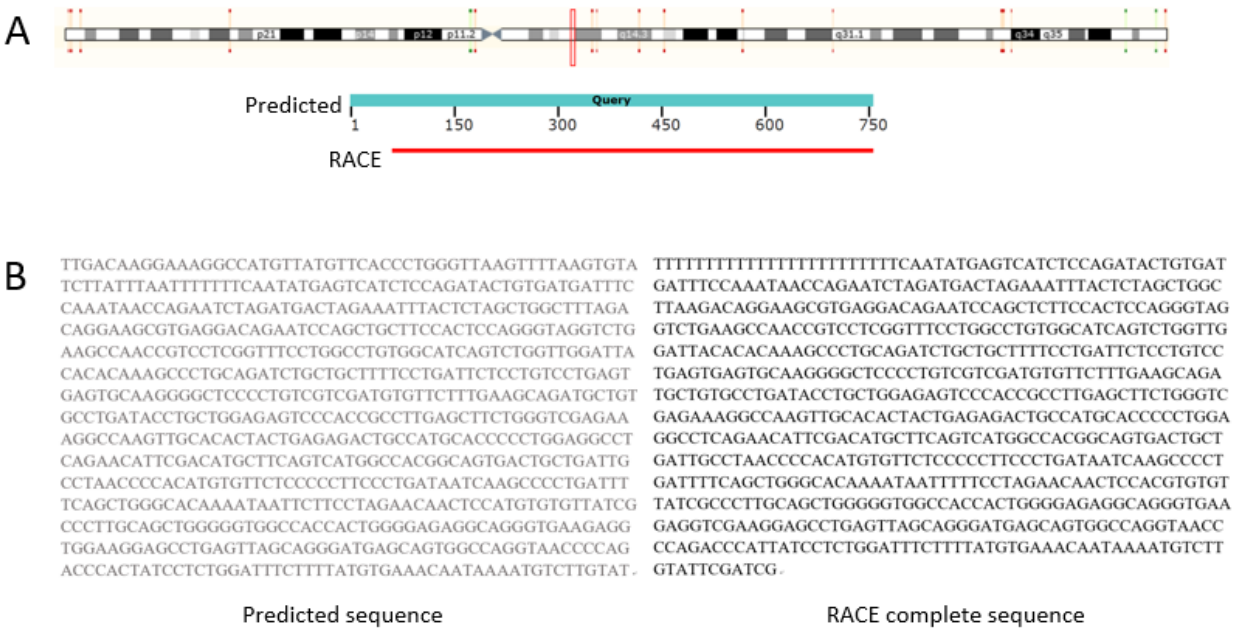

Figure 2.2.1.1: Full-length sequence of AC017002.3 was validated. (A) Length of RACE-verified AC017002.3 was compared to predicted AC017002.3 sequence on Ensembl.org. (B) Sequences of RACE-verified and predicted AC017002.3 on Ensembl.org.

with ATGG or ATGGG insertion at the beginning. If AC017002.3 has any open reading frame (ORF) in the sense or antisense direction, or cryptic ORFs out of frame with any endogenous start codon, the encoded peptide, fused with a FLAG tag, would be expressed and detectable by an anti-FLAG antibody. AC017002.3 has a length of 719 nucleotides, and thus the largest peptides potentially encoded by AC017002.3 would be around 30 kDa in size. The above described constructs were transfected in HeLa and allowed to express for 48 h, along with FLAG-fused HIV protein Vpr as a positive control. Presence of FLAG-fused proteins were probed by western blotting. While proteins up to 40 kDa could be detected, only FLAG-Vpr was immunoblotted (Figure 2.2.1.2). This result shows that AC017002.3 is a *bona fide* non-coding RNA.

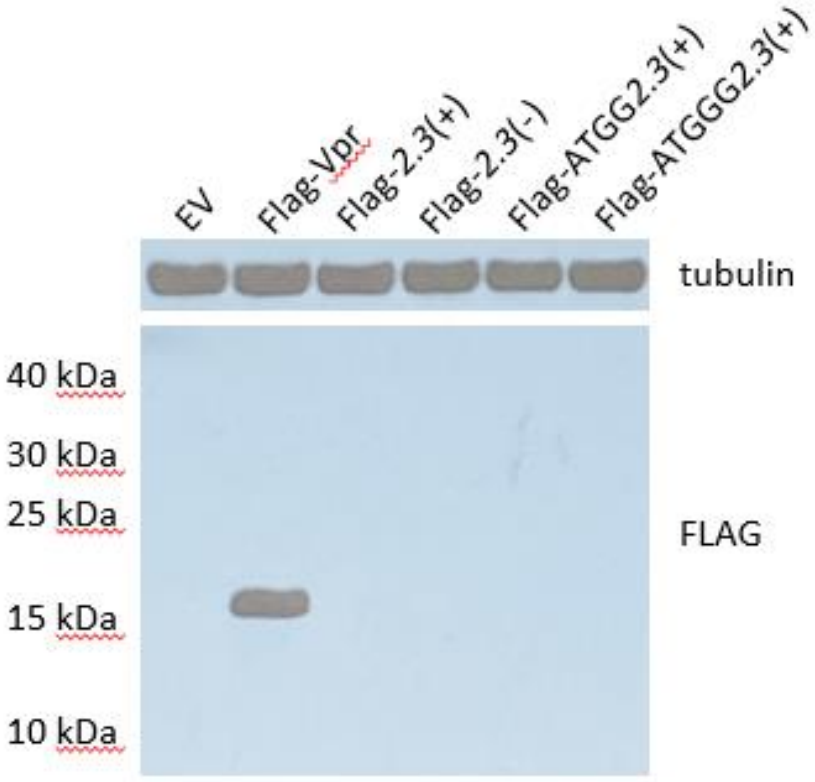

Figure 2.2.1.2 AC017002.3 is a *bona fide* non-coding RNA. AC017002.3 complete sequence was cloned into pFLAG-CMV in the indicated forms and transfected into HeLa cells along pFLAG-CMV empty vector and pFLAG-Vpr. 48 h post-transfection, expression of FLAG-fused proteins was detected by western blotting. HIV Vpr was probed as a positive control. From left to right: empty vector; FLAG-fused Vpr; AC017002.3 sense sequence; AC017002.3 antisense sequence; AC017002.3 sense sequence with an insertion of ATGG at the beginning; AC017002.3 sense sequence with ATGGG insertion at the beginning.

The localization of lncRNAs affects their function and informs strategy for loss-of-function editing. Therefore, the relative distribution of AC017002.3 in the nucleus versus in the cytoplasm was examined. Doxycycline-induced iSLK cells were fractionated into nuclear and cytoplasmic portions. An equal number of cells was lysed to make whole-cell lysates, which served as input. Nuclear marker lamin A/C and cytoplasmic marker GAPDH were immunoblotted to show the success of fractionation (Figure

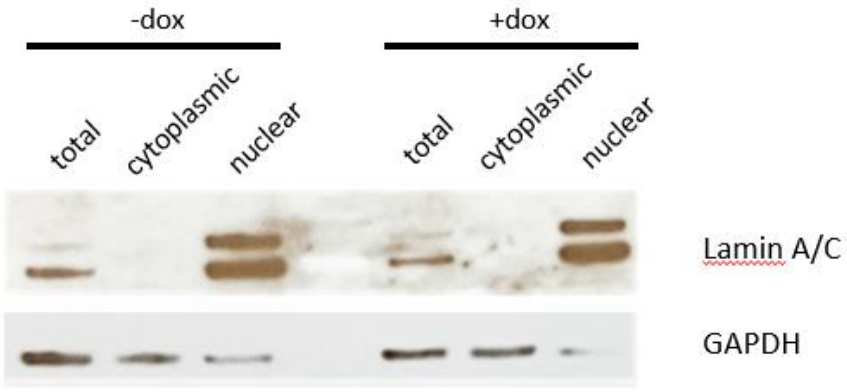

2.2.1.3). The levels of AC017002.3 in the nucleus and the cytoplasm

Figure 2.2.1.3 Successful cell fractionation was verified by immunoblotting nuclear and cytoplasmic markers. Mock- or doxycycline-induced iSLK cells were fractionated, and equal amounts of nuclear and cytoplasmic fractions were subject to western blotting, with equal amounts of whole-cell lysates as input.

Graph 2.2.1 AC017002.3 is almost exclusively present in the nucleus. iSLK cells were doxycycline-induced for 48 h, fractionated into nuclear and cytoplasmic portions, and the levels of AC017002.3 transcripts in the fractions were quantified by qPCR. The Ct values of AC017002.3 in the nuclear and cytoplasmic fractions were compared to that in the input, which is whole-cell lysate from the same number of iSLK cells that were fractionated. Bar represents mean ± SD. N = 4.

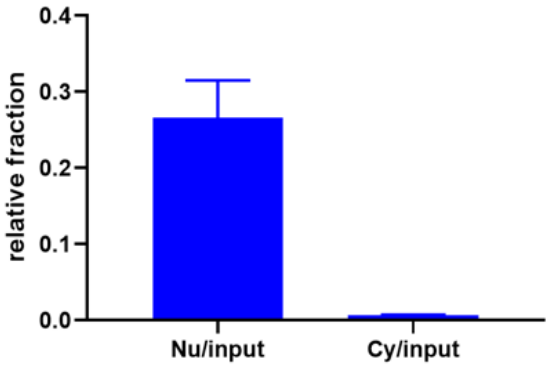

were quantified by qPCR and by comparison to AC017002.3 levels in inputs. Graph 2.2.1 shows that AC017002.3 is almost exclusively present in the nucleus. This result suggests that AC017002.3 may function in the nucleus and interact with nuclear proteins, thus informing the strategy for later study of its mechanism.

2.2.2 AC017002.3 Positively Regulates KSHV Early Gene Expression

To functionally characterize AC017002.3 in the context of KSHV lytic reactivation, stable A017002.3 knock-down cell line was established using CRISPR interference (CRISPRi). The CRISPR technology is derived from a prokaryotic antiviral system mediated by CRISPR-associated proteins (Cas) that silences foreign nucleic acids with viral origins (Barrangou et al., 2007). Although endogenous CRISPR requires CRISPR RNA (crRNA) and *trans*-acting RNA (tracrRNA) to direct Cas9 endonucleases, targeted silencing by CRISPR in the cell only requires an engineered single guide RNA (sgRNA) that contains a linker, holding together a crRNA-tracrRNA chimera (Deltcheva et al., 2011; Jinek et al., 2012). sgRNA complexes with Cas9 and directs it to the target double-stranded DNA

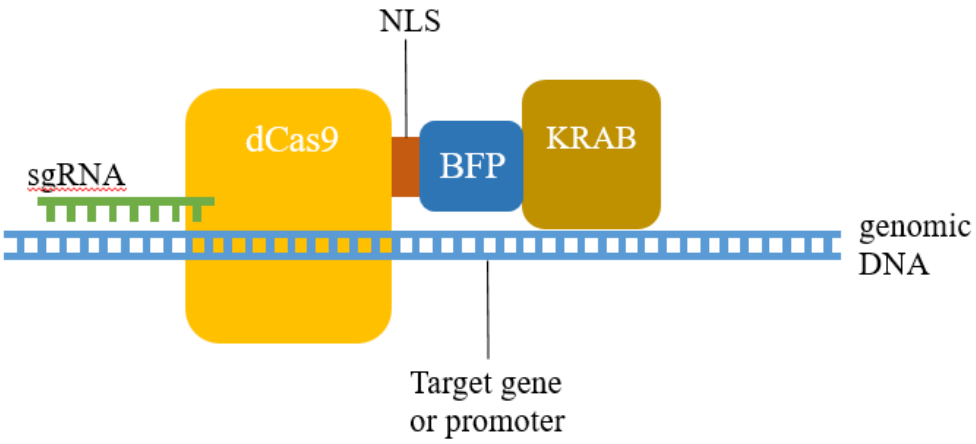

Figure 2.2.2.1: CRISPRi system used in this study. dCas9 is fused with BFP and the repressive chromatin modifying domain KRAB. When both the dCas9-KRAB chimera and sgRNAs are expressed, sgRNA guides dCas9-KRAB to specific target genes or promoters, and transcriptional activity is suppressed via the KRAB domain.

(dsRNA) site according complementary base pairing, where Cas9 recognizes a GG dinucleotide known as the protospacer adjacent motif (PAM) sequence (Jinek et al., 2012). CRISPRi is a variant of the above described CIRPSR knock-out (KO) technique. It utilizes a catalytically inactive Cas9, or dead Cas9 (dCas9), to sterically block RNA polymerase, or to functionally suppress transcription wherein the dCas9 is fused with an effector domain of a repressive transcription factor, such as the Krüppel associated box (KRAB) domain (Figure 2.2.2.1) (Gilbert et al., 2013).

To prepare for CRISPRi, stable dCas9-KRAB overexpression iSLK cell line was established. pHR-SFFV-dCas9-BFP-KRAB was packaged into lentiviral vectors and transduced into iSLK cells. Transduction was performed twice to ensure transduction efficiency and enable high expression of dCas9-KRAB in cells transduced by multiple lentiviral particles. Cells were then FACS sorted to isolate a BFP+ subpopulation (Graph 2.2.2.1). iSLK-KRAB cells were expanded and maintained.

Graph 2.2.2.1 iSLK cells stably expressing BFP from pHR-SFFV-dCas9-BFP-KRAB were FACS-sorted. DNase and Accumax (Stem Cell Technologies) were added to ensure cells remain single.

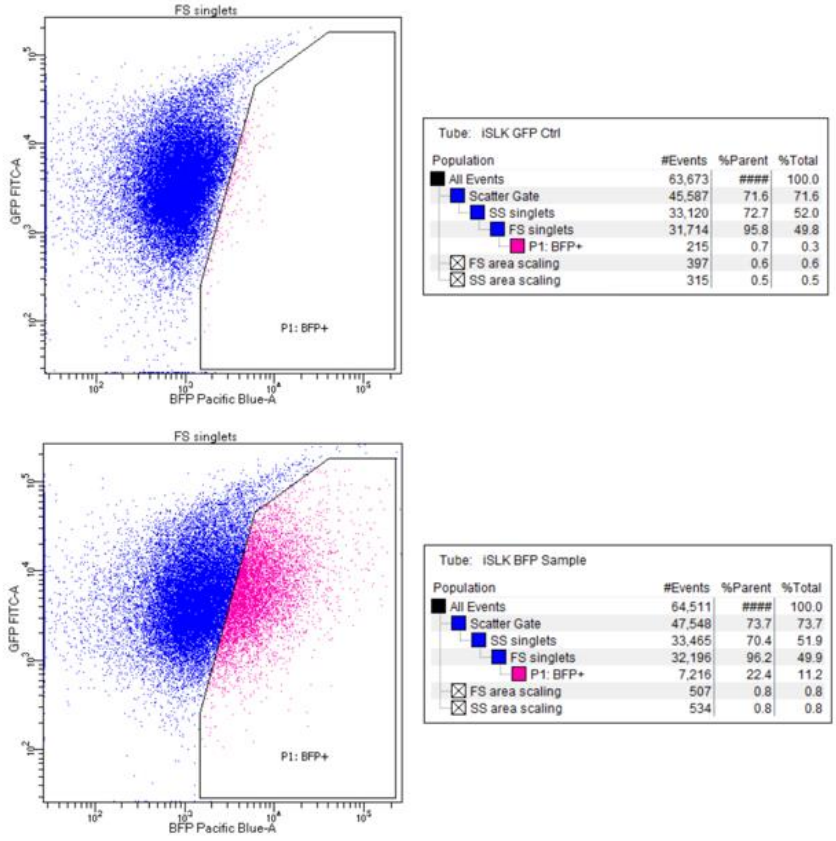

Knock-down of AC017002.3 was achieved by transducing lentiviral vectors carrying sgRNA expressing cassettes. Two different sgRNAs were employed to account for possible off-target effects (Table 2.2.2). Knock-down cell lines were induced by doxycycline, and early lytic gene expression, as well as knock-down efficiency, was assessed by qPCR. Possibly due to relatively low basal expression, oppositional induction upon doxycycline treatment, or low accessibility of chromatin in the predicted promoter area, the knock-down efficiency of AC017002.3 was modest but still significant, approxiamtely 25% to 35% (Graph 2.2.2.2 A). However, the levels of early lytic transcripts PAN and K8 were both

Graph 2.2.2.2 AC017002.3 knock-down decreases KSHV early gene expression. Stable AC017002.3 CRISPRi knock-down cell lines, as well as non-targeting control (NTC) cell lines, were established and induced with 1 μg/mL doxycycline. Total RNA was extracted 30 h post-induction and KSHV early gene expression, as well as AC017002.3 transcript levels, was quantified by qPCR. Shown are knock-down efficiency at the point of sample collection (A), and relative transcript levels of PAN (B) and K8 (C). Bar represents mean ± SD. **p*<0.05, ***p*<0.01, ****p*<0.001, *****p*<0.0001, by Student's *t* test. N = 4.

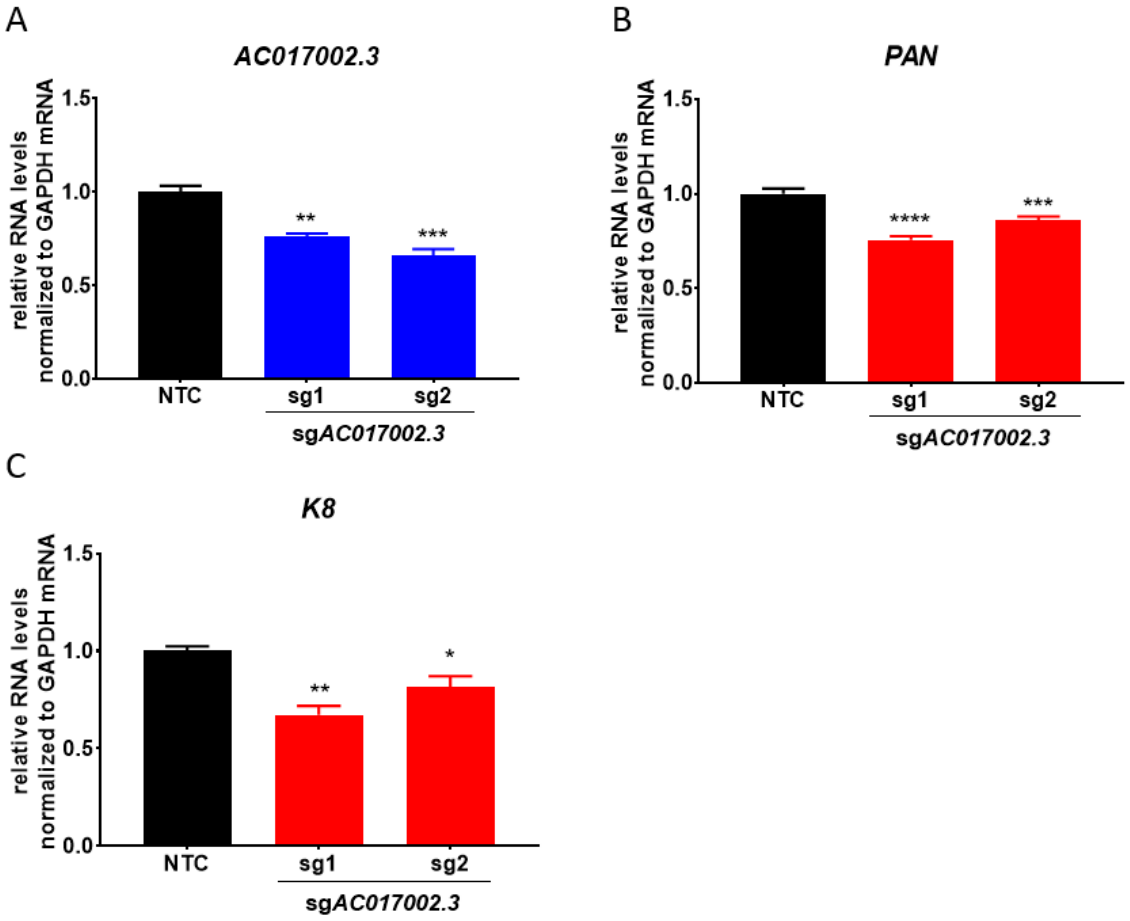

significantly decreased in knock-down cells compared to control, with PAN decreasing by approximately 15% to 25% (Graph 2.2.2.2 B and C). In accordance with these observations, the protein level of K8 was also downregulated (Figure 2.2.2.2). Therefore, these results, combined with the knowledge that PAN is induced to very high levels, suggest a biologically meaningful role for AC017002.3 in positively regulating KSHV early lytic gene expression during reactivation.

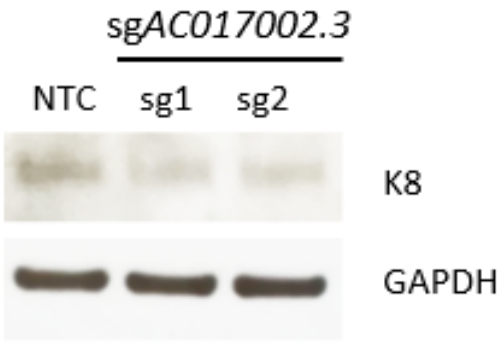

Figure 2.2.2.2 AC017002.3 knock-down decreases the level of KSHV early protein K8. AC017002.3 CRISPRi knock-down iSLK cells, as well as NTC cells, were induced with 1 μg/mL doxycycline. 24 h post-induction, cells were lysed, and K8 protein level was detected by western blotting.

Table 2.2.2 Seed sequences used to construct sgRNAs targeting the promoter region of *AC017002.3*.

	Seed sequence
sgNTC	ACGGAGGCTAAGCGTCGCAA
sg*AC017002.3*-1	AGGCCATGTTATGTTCACCC
sg*AC017002.3*-2	GCAGAATGGAAGAGAGCATC

To corroborate the functional assessment of AC017002.3 by CRISPRi knock-down, AC017002.3 was overexpressed in iSLK cells and changes in early lytic gene expression was examined. Upon lentiviral transduction, iSLK cells were allowed 2 days to overexpress AC017002.3 prior to doxycycline treatment. Overexpression efficiency was high (Graph 2.2.2.3 A). As expected, AC017002.3 overexpression upregulated PAN and K8 at the transcript level, and K8 at the protein level (Graph 2.2.2.3

B and C, Figure 2.2.2.3). These data confirm that AC017002.3 is a positive regulator of KSHV early lytic gene expression.

Graph 2.2.2.3 AC017002.3 overexpression increases KSHV early gene expression. iSLK cells were transduced with lentivirus carrying pLVX-*AC017002.3*. 48 h post-transduction, cells were induced with 0.1 µg/mL doxycycline. At indicated time points post-induction, total RNA was extracted and KSHV early gene expression, as well as AC017002.3 transcript levels, was quantified by qPCR. Shown are overexpression efficiency at the point the sample collection (A), and relative transcript levels of PAN (B) and K8 (C). Bar represents mean ± SD. **p*<0.05, ***p*<0.01, ****p*<0.001, by Student's *t* test. N =4.

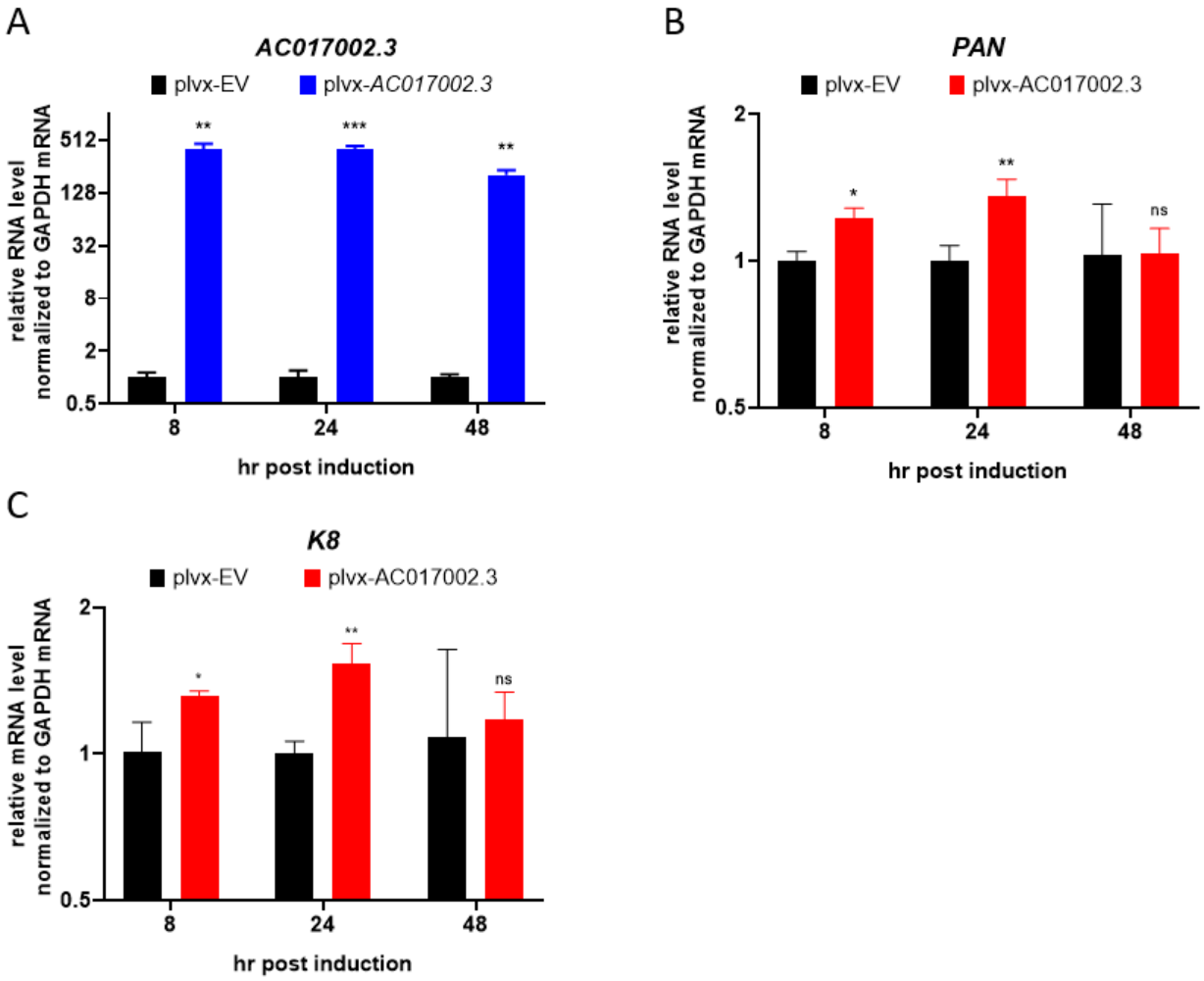

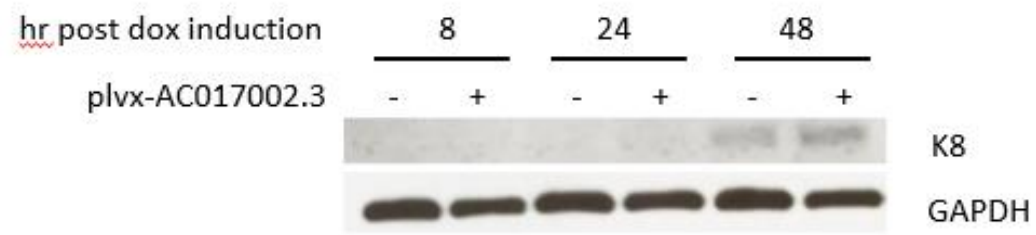

Figure 2.2.2.3 AC017002.3 overexpression increases the level of K8 protein. iSLK cells were transduced with lentivirus carrying pLVX-*AC017002.3* or empty vectors. 48 h post-transduction, cells were induced by 0.1 μg/mL doxycycline. At indicated time points post-induction, cells were lysed, and K8 protein level was detected by western blotting.

2.3 Mechanism of AC017002.3 Function

2.3.1 AC017002.3 Interacts with Nuclear Proteins

LncRNAs often interact with proteins to exert functions. To reveal clues to how AC017002.3 functions, its interacting partners were searched for through RNA affinity pull-down. Proteins that interact with biotinylated *in vitro* transcribed AC017002.3 can be isolated by using streptavidin-coated beads to precipitate the RNA, and subsequently identified via mass spectrometry (Figure 2.3.1.1). To account for the noise generated by the ability of RNA-binding proteins to bind RNA nonspecifically, *LacZ* mRNA, which is not present physiologically in human cells, was used as a negative control (Figure 2.3.1.2). Because AC017002.3 is almost exclusively present in the nucleus, only nuclear proteins were used in the pull-down. Mock- or doxycycline-treated iSLK cells were fractionated into nuclear and cytoplasmic fractions. Nuclear protein concentration was measured and mixed with biotinylated AC017002.3 or *LacZ* mRNA, prior to pull-down by streptavidin beads. Proteins were then denatured and separated by SDS-PAGE. Silver staining revealed bands of proteins associated with the RNAs (Figure 2.3.1.3A). Multiple bands were specifically enriched by AC017002.3 (Figure 2.3.1.3B). To

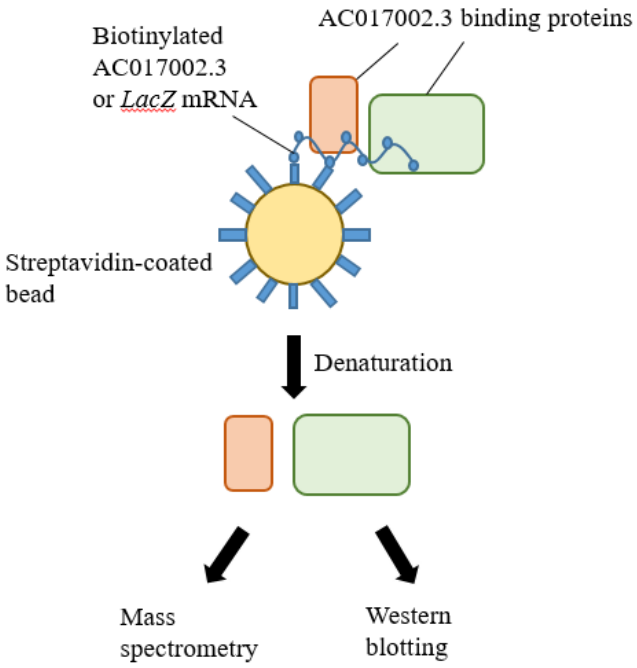

Figure 2.3.1.1 RNA affinity pull-down. Biotinylated *in vitro* transcribed RNA is allowed to interact with proteins in cellular lysates. Beads coated with streptavidin interact with biotin and precipitate the RNA along with bound proteins. After interactions are destroyed by denaturing the pull-down complex, proteins may be subject to mass spectrometry or western blotting.

identify proteins that associate with AC017002.3, samples of affinity pull-down were analyzed by mass spectrometry. Three categories of candidates of AC017002.3 interacting partners were uncovered: those enriched in both mock- and doxycycline-treated iSLK cells, and those enriched in doxycycline-treated cells only, and those enriched in mock-treated cells only (Graph 2.3.1.1).

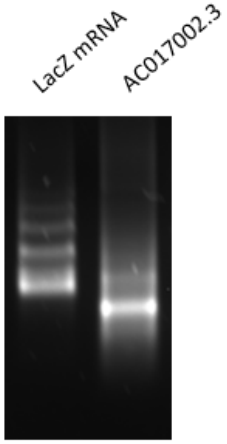

Figure 2.3.1.2 *in vitro* transcribed AC017002.3 and *LacZ* mRNA are largely undamaged. pBluescript KSII vectors carrying AC017002.3 and *LacZ* mRNA sequences were digested by KpnI and examined by 2% agarose gel electrophoresis.

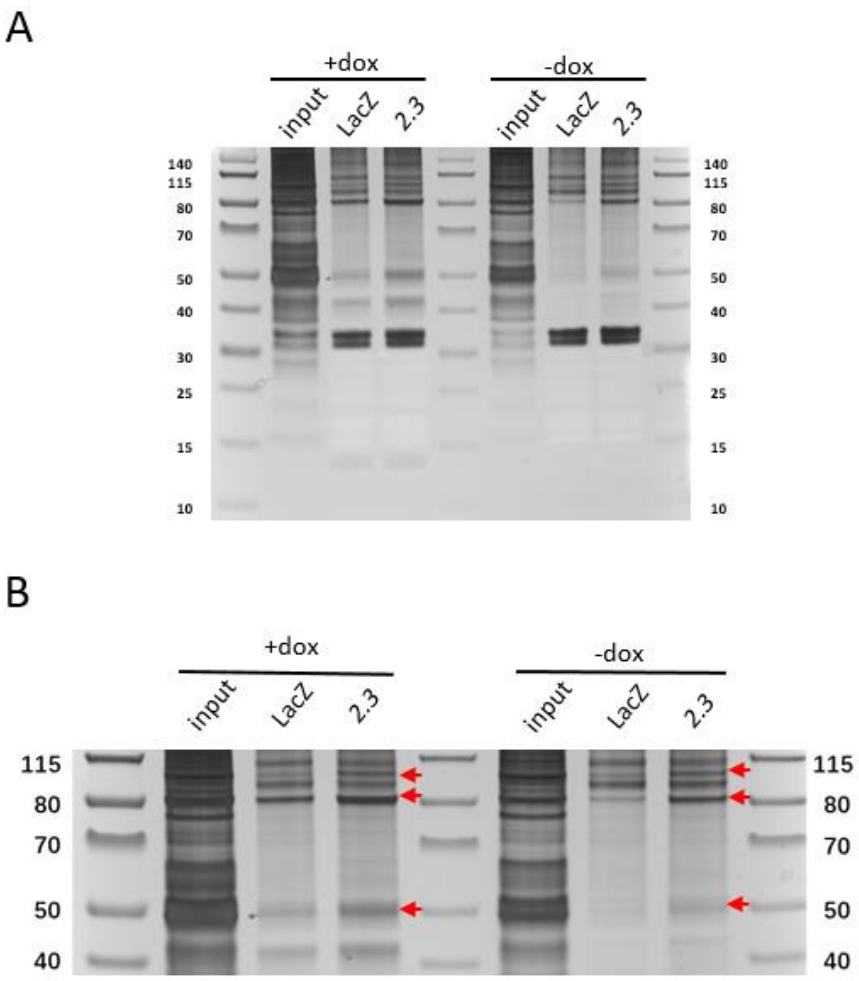

Figure 2.3.1.3 AC017002.3 specifically interact with nuclear proteins. Nuclear lysates prepared from mock- or doxycycline-induced iSLK cells were incubated with *in vitro* transcribed AC017002.3 and *LacZ* mRNA with streptavidin magnetic beads. After three washes, proteins were dissociated from beads and denatured, and subject to SDS-PAGE. Protein bands were visualized by silver staining (A). Some bands specifically enriched by AC017002.3 were highlighted (B).

2.3.2 hnRNP K and ILF2 are AC017002.3 Interacting partners

Western blotting was performed using pull-down lysates to verify candidate proteins identified in mass spectrometry. hnRNP K, a nuclear RNA binding protein, and ILF2, subunit of a transcription factor, were found to be consistently enriched (Figure 2.3.2).

Graph 2.3.1 Identification of nuclear proteins that interact with AC017002.3. *In vitro* transcribed, biotinylated AC017002.3 and *LacZ* mRNA were incubated with nuclear lysates prepared form mock- or doxycycline-induced (1 µg/mL) iSLK cells. Pull-down fractions were analyzed by mass spectrometry. Proteins enriched by AC017002.3 in both mock- and doxycycline-induced samples (A), in doxycycline-induced samples only (B), and in mock-induced samples only (C) are shown. Bar represents mean ± SD. N = 2.

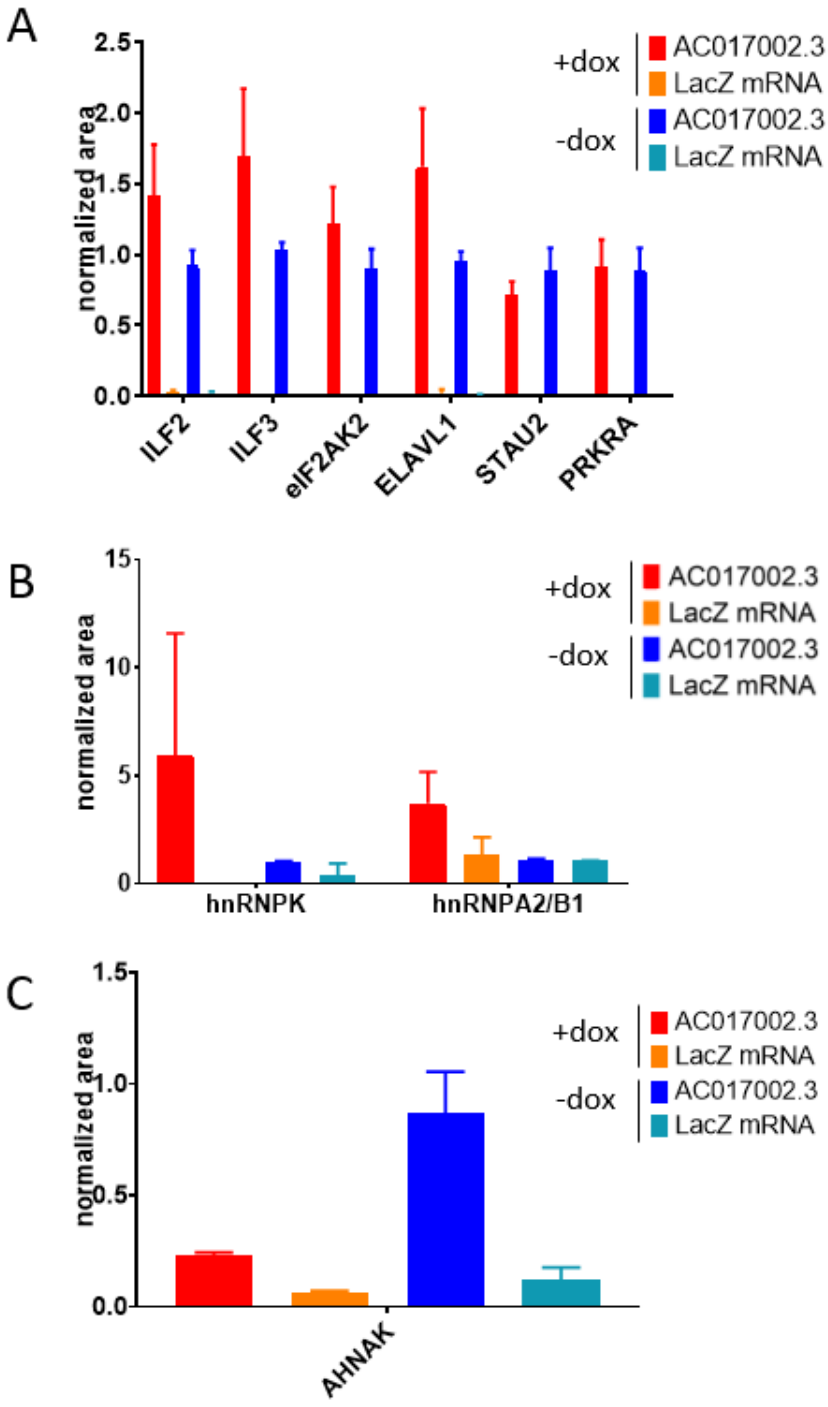

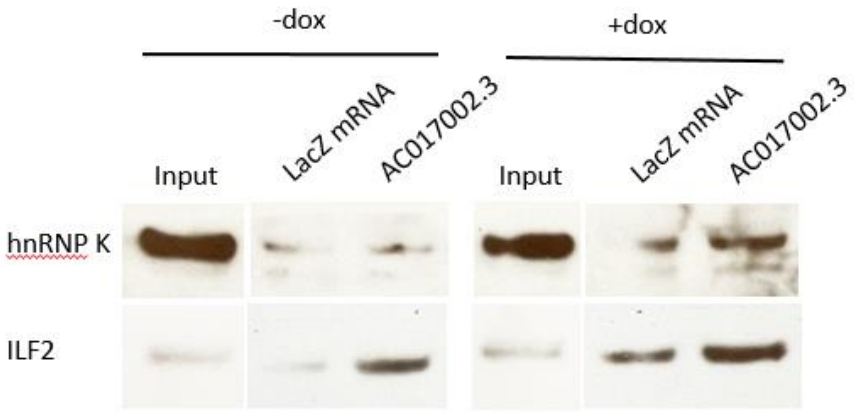

Figure 2.3.2 AC017002.3 specifically interacts with hnRNP K and ILF2. AC017002.3 affinity pull-down was performed with *LacZ* mRNA as control. AC017002.3-interacting proteins were detected by western blotting.

Chapter 3: Discussion and Future Perspectives

KSHV is an oncogenic virus associated with multiple malignancies, typically found in immunosuppressed individuals. Its life cycle has two genetically distinct phases, and switching between them involves intricate regulatory networks. lncRNAs comprise a largely unexplored host regulatory module, and have been shown to function in the life cycles of many viruses. However, whether and how lncRNAs function in KSHV lytic reactivation are unknown. In this study, the lncRNA landscape during KSHV lytic reactivation was described through RNA-seq, where many novel transcripts were found to be differentially expressed. One of these novel lncRNAs, AC017002.3, was studied, and its full-length sequence was produced by RACE. AC017002.3 is a nuclear transcript devoid of coding potential, and it positively regulates KSHV early transcript levels in doxycycline-induced iSLK cells. AC017002.3 interacts with the nuclear proteins hnRNP K and ILF2, suggesting a ribonucleoprotein complex-based regulatory mechanism.

In the functional knock-down experiment, the fold change of the lytic genes is only modest. However, two reasons suggest that the observed change is still likely biologically meaningful. First, knock-down efficiency of AC017002.3 was similarly modest, and thus a modest phenotype was expected. Second, upon induction, the transcript level of PAN in iSLK cells could readily surpass that of GAPDH mRNA by approximately 10 folds 30 h post-doxycycline treatment, becoming extremely abundant and accounting for the vast majority of both viral lytic transcripts and total cellular polyadenylated transcripts during KSHV reactivation (Arias et al., 2014; Conrad, 2016). At the peak of lytic replication, the copy number of PAN RNA could average 10^5 copies per cell (Zhong et al., 1996). Thus, even a 15% to 25% decrease would mean the depletion of a number of PAN transcripts higher than the copy numbers of the majority of polyadenylated RNAs in the cell.

Two interacting partners of AC017002.3, hnRNP K and ILF2, were verified. hnRNP K has been shown to interact with the viral ORF57 protein (Malik and Clements, 2004). ORF57 is a multifunctional early protein with documented roles in RNA stabilization, especially PAN RNA, splicing of viral pre-

mRNAs, and destabilization of host genome (Jackson et al., 2014; Majerciak et al., 2008; Massimelli et al., 2011). hnRNP K is also a multifunctional protein with documented functions in transcriptional activation, post-transcriptional processing, and translational control (Cao et al., 2012; Liepelt et al., 2014; Moumen et al., 2005; Tsai et al., 2013). The functionality of its interaction with hnRNP K is currently unclear. However, the segments of hnRNP K required for interaction with ORF57 and ICP27, an ORF57 homologue in herpes simplex virus type 1 (HSV-1), overlap, and hnRNP K-complexed ORF57 and ICP27 are both phosphorylated by casein kinase 2 (CK2), which is present in both complexes (Malik and Clements, 2004). This suggests that hnRNP K interaction with the ICP27 family protein of alphaherpesvirinae and gammaherpesvirinae is conserved, and that the interaction is likely functional.

ILF2 is a transcription factor that regulates immediate early gene expression (Wu et al., 2019). There is currently no clear connection between ILF2 and KSHV lytic reactivation.

For future investigation of hnRNP K-related mechanism, hnRNP K-ORF57 interaction and ORF57-AC017002.3 interaction in doxycycline-induced iSLK cells could first be examined by co-immunoprecipitation and RNA affinity pull-down. If the interactions are verified, the role of AC017002.3 in those interactions could be tested by co-immunoprecipitation in knock-down or overexpression cells. Finally, the functionality of hnRNP K-ORF57 interaction may be studied by mutating the ORF57 binding region in hnRNP K and examining the effects on KSHV reactivation. Future study of the ILF2-AC017002.3 complex could focus on the potential role of ILF2 in the transcriptional regulation of viral genes. Chromatin isolation by RNA purification (ChIRP) could be used to examine AC017002.3 binding to the promoters of *PAN* and *K8*, and chromatin immunoprecipitation (ChIP) could be used to detect ILF2 binding to these promoters.

KSHV is a complex DNA virus with a biphasic life cycle. The latent-to-lytic switch of KSHV is pathologically important but the host-virus regulatory network involved in this process still needs exploration. This study uncovered the long non-coding transcriptome during KSHV reactivation and characterized a novel lncRNA, AC017002.3, as a positive regulator of viral early lytic genes, including *PAN* and *K8*. Both PAN and K8, previously shown to regulate the expression of many other lytic genes,

are essential for robust lytic reactivation (Liao et al., 2003; Rossetto et al., 2013). Therefore, this study reveals a biologically significant role for AC017002.3 in regulating KSHV lytic reactivation, providing the first evidence that host lncRNAs are involved in modulating the KSHV latent-to-lytic switch.

Chapter 4: Materials and Methods

4.1 Cell Culture and Media

Medium A: DMEM (Gibco) supplemented with 10% fetal bovine serum (FBS).

Medium B: DMEM supplemented with 10% FBS, 800 µg/mL G-418 (Gibco), 1200 µg/mL hygromycin B (Thermo Fisher Scientific), and 10 µg/mL puromycin (Alfa Aesar).

293FT and HeLa cells were cultured in medium A. Cryo-preserved iSLK cells were recovered in medium A. The next day, medium was changed to medium B, in which iSLK cells were maintained. BC-3-G cells were cultured in RPMI 1640 (Gibco) supplemented with 10% fetal bovine serum (FBS), 100U/mL Penicillin and streptomycin, and 1.5 µg/mL puromycin.

4.2 Induction of KSHV Lytic Reactivation

For the induction of KSHV in iSLK cells, cells were seeded in medium A. The next day, doxycycline stock was diluted to indicated concentrations in medium A, and culture medium was changed to doxycycline-supplemented medium A, in which cells were maintained for indicated lengths of treatment.

For the induction of KSHV in BC-3-G cells, cells were seeded in RPMI 1640 supplemented with indicated concentrations of TPA and treated for indicated time periods.

4.3 Library preparation and RNA-seq

iSLK cells and BC-3-G cells were treated with 1 µg/mL doxycycline and 20 ng/µL TPA, respectively, for 48 h. Cells were lysed and total RNA was extracted, treated with TURBO DNase (Thermo Fisher Scientific) according to the manufacturer's instructions. Approximately 0.6 µg RNA per sample was depleted of ribosomal RNA using RobiMinus kit (Life Technologies). Library was prepared and sequenced by IGM Core.

4.4 Rapid Amplification of cDNA Ends

Total RNA extracted from doxycycline-treated iSLK cells was depleted of ribosomal RNA with RiboMinus kit (Life Technologies). RACE was performed with SMARTer RACE kit (Clonetech) according to the manufacturer's instructions. Briefly, approximately 100 ng purified poly(A) RNA was used for each reverse transcription reaction to produce cDNA, which served as template in nested PCRs to amplify target lncRNA cDNA ends. RACE PCR products were cloned using Zero Blunt TOPO cloning kit (Thermo Fisher Scientific) and transformed into Stellar competent cells (Takara). Viable colonies on ampicillin+ agar LB plates were expanded and subject to plasmid extraction. Plasmids were then sequenced. The 5 prime and 3 prime ends of AC017002.3 were aligned with the predicted sequence of AC017002.3 on Ensembl.org.

4.5 Lentivirus Production

Lentiviral expression plasmids were transformed into Stellar competent cells (Takara). Transformed colonies that grew on LB agar plates containing ampicillin were expanded, and subsequently extracted for plasmids using Qiaprep Spin Miniprep kit according to the manufacturer's protocol.

Lentiviruses were produced in 293FT cells using Lipofectamine 3000 (Invitrogen) according to the manufacturer's instructions. Briefly, 10^6 cells were seeded per well in 6-well plates 1 day prior to transfection. The next day, lentiviral packaging vectors (Systems Biosciences), along with lentiviral expression plasmids, were transfected into the cells. Medium was changed 6 h post-transfection. 48 h post-transfection, virus-harboring supernatants were collected and centrifuged to remove cellular debris.

4.6 Generation of iSLK-KRAB Population

pHR-SFFV-dCas9-BFP-KRAB (Addgene 46911) was packaged into lentiviral particles, which were transduced into iSLK cells. BFP+ population of iSLK was sorted by FACS. The iSLK-KRAB population was maintained in medium B.

4.7 Lentivirus-mediated knock-down and overexpression

Complete sequence of AC017002.3 was cloned into pLVX-Puro (Clonetech) to generate pLVX-AC017002.3. sgRNA oligonucleotides were annealed and cloned into lenti-sgRNA blast (Addgene

104993) according to Zhang lab's protocol (PMC5526071). Plasmids were packaged into lentiviral particles as described above. Lentivirus for pLVX-AC017002.3 was transduced into iSLK cells, and Lentivirus for sgRNA knock-down was transduced into iSLK-KRAB cells. Transduction of iSLK cells was performed with 8 μg/mL polybrene (Millipore) in medium A, and cell-virus mixture was centrifuged at 750 *g* for 45 min to enhance transduction efficiency. The next day, medium was changed to medium B. For stable knock-down cell line construction, 15 μg/mL blasticidin (Alfa Aesar) was added to the medium and transduced cells were selected for at least 5 days.

4.8 RNA Extraction and Real-time PCR

Total cellular RNA was extracted using TRIzol reagent (Invitrogen) according to the manufacturer's instructions. RNA was reverse transcribed with iScript Reverse Transcription Supermix (BioRad) to generate cDNA, which was subsequently subject to qPCR using SsoAdcanved SYBR Green Mix (BioRad). Fold change in gene expression was calculated using ΔΔCt and normalized to glyceraldehyde 3-phosphate dehydrogenase (*GAPDH*) mRNA.

Table 4.8: qPCR primers.

Gene name	Forward primer	Reverse primer
AC017002.3	GTAGGTCTGAAGCCAACCGT	CCAACCAGACTGATGCCACA
PAN	AGGCGACAAAGTGAGGTG	ACATTGAAAGAGCGCTCC
K8	TGCGTCTGTAGTTAAGGCCG	CGTATCTGCCTTGCTTTCGC
MPRIP-AS1	AACAGAGGAGCAGCAAGACC	AGTGGTCTGGCTTTTGGAGG
AC133644.2	AAAGAAAGACCCTCGGCAGG	TTTGCTGGTTCCCAAGAGCA
KCNMA1-AS1	TCTTCCCAACCTGCCAAGAC	GTTCCTCCCAATGTCCCCAG
AL591178.1	CCCCTCGATCGTCAGAAACC	CACCACCATCGCTCATCCTT
KCNMA1-AS3	AGGCAGTGATTGCTTCCAGT	ATCTCCATCGCAGCCATTCC
HPYR1	CAGTTTCCCCAGGTTCTGCT	AGAGTGGTGGCTCAGAGGAT
AC009226.1	GCATAAGCTGTCCTGGGTGT	TGGTGGGATCTGGAAGAAGC
LINC01943	AAGCAGATGCTGTGCCTGAT	GTGCATGGCAGTCTCTCAGT
AP000779.1	GCATGGGATACTTCCTGCCA	TTCTCCATGGCCAACTCTGC
AL138689.2	CAATTCTCCAGGTCAGCGGT	CAGGCCCTTTGAAGGTTTGC

Gene name	Forward primer	Reverse primer
AL157392.3	CAAGGACCACCGCCTACTTT	GGGTTCATCACTGGGAGGTG
AC079601.1	GGAATCATCATCCTCGCCGT	CCCGGGAGATCCAAGCATAC

4.9 Western Blot and Antibodies

Cells were lysed with Pierce IP lysis buffer (Thermo Fisher Scientific), supplemented with protease inhibitor cocktail (RPI). Protein concentration was measured using DC protein assay (BioRad). Proteins were denatured, separated on NuPage 4-12% Bis-Tris Gel (Invitrogen), and transferred to PVDF membrane (BioRad). Immunoblotting was performed using Fast Western Blot kit (Thermo Fisher Scientific) according to the manufacturer's protocol. Antibodies used are mouse anti-FLAG M2 (Sigma, F1804), rabbit anti-GAPDH (Cell Signaling Technology, 2118), HRP-conjugated mouse anti-tubulin (Proteintech, HRP-66031), goat anti-lamin A/C (Santa-Cruz, sc-6215), mouse anti-K8α (Santa-Cruz, sc-57889), mouse anti-hnRNP K (Abcam, ab39975), rabbit anti-ILF2 (Abcam, ab154169).

4.10 Cell Fractionation

Cells were trypsinized and resuspended in plasma membrane lysis buffer consisting of 10 mM Tris-HCl (pH 7), 1.5 mM $MgCl_2$, 10 mM KCl, 0.5 mM DTT, and 0.25% NP-40, supplemented with PMSF and protease inhibitor cocktail. 10 mL plasma membrane lysis buffer was added per 10^7 cells, and lysis reaction proceeded on a rocker at 4°C for 10 min. Upon the completion of plasma membrane lysis, reactions were centrifuged at 2500*g* for 15 min at 4°C. Supernatants containing cytoplasmic fractions were stored at -80°C. Nuclear pellets were resuspended in nuclear membrane lysis buffer consisting of 25 mM Tris-HCl (pH 7), 150 mM KCl, 0.5 mM DTT, and 0.5% NP-40, supplemented with PMSF and protease inhibitor cocktail. Nucleus suspension was homogenized with a syringe and centrifuged at 13000 rpm for 10 min at 4°C. Nuclear fractions were collected and stored at -80°C. For detection of GAPDH and lamin A/C, protein concentrations of both fractions were measured by DC protein assay, and equal amounts of cytoplasmic and nuclear lysates were used in western blotting.

4.11 RNA Affinity Pull-down

AC017002.3 and *LacZ* mRNA sequences were separately cloned into the downstream of the T7 promoter in pBluescript KSII vectors. KpnI (New England BioLabs) was used to digest the vectors. Linear fragments containing AC017002.3 and *LacZ* served as template for *in vitro* transcription and biotinylation with mMESSAGE mMACHINE T7 Transcription kit (Invitrogen) according to the manufacturer's instructions with modifications. Integrity of the RNA were analyzed by 2% agarose gel electrophoresis.

For RNA affinity pull-down, 2 µg RNA was *in vitro* folded. Briefly, RNA was diluted to 200 ng/µL in 1x NEBuffer 2 (New England BioLabs), heated to 60°C for 10 min, and cooled down to 4°C at a ramp rate of -1°C/min. Pierce streptavidin beads (Thermo Fisher Scientific) were washed in nuclear membrane lysis buffer, described in Cell Fractionation, and used to clear nuclear lysates prepared from mock- or doxycycline-treated iSLK cells. 1 mg nuclear lysate was incubated with 2 µg folded RNA and 40 µL streptavidin beads for 2 h at 4°C. Beads were collected, washed three times with nuclear membrane lysis buffer, and either sent to Biomolecular & Proteomics Mass Spectrometry Facility at UCSD for analyses by mass spectrometry, or treated to denature the proteins for SDS-PAGE. Silver staining was performed using Pierce Silver Stain kit (Thermo Fisher Scientific) according to the manufacturer's instructions.

4.12 Statistical Analysis

Volcano plots were generated using R Studio. Other graphs were generated using GraphPad Prism 8.0.2 (GraphPad Inc.). Statistical analysis was performed by student's t-test (paired, two-sided).

References

Aneja, K.K., and Yuan, Y. (2017). Reactivation and Lytic Replication of Kaposi's Sarcoma-Associated Herpesvirus: An Update. Front Microbiol *8*, 613.

Arias, C., Weisburd, B., Stern-Ginossar, N., Mercier, A., Madrid, A.S., Bellare, P., Holdorf, M., Weissman, J.S., and Ganem, D. (2014). KSHV 2.0: a comprehensive annotation of the Kaposi's sarcoma-associated herpesvirus genome using next-generation sequencing reveals novel genomic and functional features. PLoS Pathog *10*, e1003847.

Balas, M.M., and Johnson, A.M. (2018). Exploring the mechanisms behind long non-coding RNAs and cancer. Non-coding RNA Res *3*, 108-117.

Barrangou, R., Fremaux, C., Deveau, H., Richards, M., Boyaval, P., Moineau, S., Romero, D.A., and Horvath, P. (2007). CRISPR provides acquired resistance against viruses in prokaryotes. Science *315*, 1709-1712.

Cao, W., Razanau, A., Feng, D., Lobo, V.G., and Xie, J. (2012). Control of alternative splicing by forskolin through hnRNP K during neuronal differentiation. Nucleic Acids Res *40*, 8059-8071.

Cesana, M., Cacchiarelli, D., Legnini, I., Santini, T., Sthandier, O., Chinappi, M., Tramontano, A., and Bozzoni, I. (2011). A long non-coding RNA controls muscle differentiation by functioning as a competing endogenous RNA. Cell *147*, 358-369.

Chai, W., Li, J., Shangguan, Q., Liu, Q., Li, X., Qi, D., Tong, X., Liu, W., and Ye, X. (2018). Lnc-ISG20 Inhibits Influenza A Virus Replication by Enhancing ISG20 Expression. J Virol *92*.

Chao, T.C., Zhang, Q., Li, Z., Tiwari, S.K., Qin, Y., Yau, E., Sanchez, A., Singh, G., Chang, K., Kaul, M., Karris, M.A.Y., and Rana, T.M. (2019). The Long Non-coding RNA HEAL Regulates HIV-1 Replication through Epigenetic Regulation of the HIV-1 Promoter. mBio *10*.

Choi, S. W., Kim, H. W., & Nam, J. W. (2019). The small peptide world in long non-coding RNAs. Briefings in bioinformatics *20*, 1853–1864.

Chatlynne, L.G., and Ablashi, D.V. (1999). Seroepidemiology of Kaposi's sarcoma-associated herpesvirus (KSHV). Semin Cancer Biol *9*, 175-185.

Clark, M.B., Amaral, P.P., Schlesinger, F.J., Dinger, M.E., Taft, R.J., Rinn, J.L., Ponting, C.P., Stadler, P.F., Morris, K.V., Morillon, A., Rozowsky, J.S., Gerstein, M.B., Wahlestedt, C., Hayashizaki, Y., Carninci, P., Gingeras, T.R., and Mattick, J.S. (2011). The reality of pervasive transcription. PLoS Biol *9*, e1000625; discussion e1001102.

Coen, N., Duraffour, S., Snoeck, R., and Andrei, G. (2014). KSHV targeted therapy: an update on inhibitors of viral lytic replication. Viruses *6*, 4731-4759.

Conrad, N.K. (2016). New insights into the expression and functions of the Kaposi's sarcoma-associated herpesvirus long non-coding PAN RNA. Virus Res *212*, 53-63.

Davis, Z.H., Verschueren, E., Jang, G.M., Kleffman, K., Johnson, J.R., Park, J., Von Dollen, J., Maher, M.C., Johnson, T., Newton, W., Jager, S., Shales, M., Horner, J., Hernandez, R.D., Krogan, N.J., and

Glaunsinger, B.A. (2015). Global mapping of herpesvirus-host protein complexes reveals a transcription strategy for late genes. Mol Cell *57*, 349-360.

Deltcheva, E., Chylinski, K., Sharma, C.M., Gonzales, K., Chao, Y., Pirzada, Z.A., Eckert, M.R., Vogel, J., and Charpentier, E. (2011). CRISPR RNA maturation by trans-encoded small RNA and host factor RNase III. Nature *471*, 602-607.

Deng, H., Young, A., and Sun, R. (2000). Auto-activation of the rta gene of human herpesvirus-8/Kaposi's sarcoma-associated herpesvirus. J Gen Virol *81*, 3043-3048.

Derrien, T., Johnson, R., Bussotti, G., Tanzer, A., Djebali, S., Tilgner, H., Guernec, G., Martin, D., Merkel, A., Knowles, D.G., Lagarde, J., Veeravalli, L., Ruan, X., Ruan, Y., Lassmann, T., Carninci, P., Brown, J.B., Lipovich, L., Gonzalez, J.M., Thomas, M., Davis, C.A., Shiekhattar, R., Gingeras, T.R., Hubbard, T.J., Notredame, C., Harrow, J., and Guigo, R. (2012). The GENCODE v7 catalog of human long non-coding RNAs: analysis of their gene structure, evolution, and expression. Genome Res *22*, 1775-1789.

Feng, J., Yang, G., Liu, Y., Gao, Y., Zhao, M., Bu, Y., Yuan, H., Yuan, Y., Yun, H., Sun, M., Gao, H., Zhang, S., Liu, Z., Yin, M., Song, X., Miao, Z., Lin, Z., and Zhang, X. (2019). LncRNA PCNAP1 modulates hepatitis B virus replication and enhances tumor growth of liver cancer. Theranostics *9*, 5227-5245.

Fortes, P., and Morris, K.V. (2016). Long non-coding RNAs in viral infections. Virus Res *212*, 1-11.

Gilbert, L.A., Larson, M.H., Morsut, L., Liu, Z., Brar, G.A., Torres, S.E., Stern-Ginossar, N., Brandman, O., Whitehead, E.H., Doudna, J.A., Lim, W.A., Weissman, J.S., and Qi, L.S. (2013). CRISPR-mediated modular RNA-guided regulation of transcription in eukaryotes. Cell *154*, 442-451.

Glaunsinger, B., and Ganem, D. (2004). Lytic KSHV infection inhibits host gene expression by accelerating global mRNA turnover. Mol Cell *13*, 713-723.

Goncalves, P.H., Ziegelbauer, J., Uldrick, T.S., and Yarchoan, R. (2017). Kaposi sarcoma herpesvirus-associated cancers and related diseases. Curr Opin HIV AIDS *12*, 47-56.

Gong, C., and Maquat, L.E. (2011). lncRNAs transactivate STAU1-mediated mRNA decay by duplexing with 3' UTRs via Alu elements. Nature *470*, 284-288.

Gossen, M., Freundlieb, S., Bender, G., Muller, G., Hillen, W., and Bujard, H. (1995). Transcriptional activation by tetracyclines in mammalian cells. Science *268*, 1766-1769.

Gradoville, L., Gerlach, J., Grogan, E., Shedd, D., Nikiforow, S., Metroka, C., and Miller, G. (2000). Kaposi's sarcoma-associated herpesvirus open reading frame 50/Rta protein activates the entire viral lytic cycle in the HH-B2 primary effusion lymphoma cell line. J Virol *74*, 6207-6212.

Grossmann, C., and Ganem, D. (2008). Effects of NFkappaB activation on KSHV latency and lytic reactivation are complex and context-dependent. Virology *375*, 94-102.

Guasparri, I., Keller, S.A., and Cesarman, E. (2004). KSHV vFLIP is essential for the survival of infected lymphoma cells. J Exp Med *199*, 993-1003.

Guttman, M., Amit, I., Garber, M., French, C., Lin, M.F., Feldser, D., Huarte, M., Zuk, O., Carey, B.W., Cassady, J.P., Cabili, M.N., Jaenisch, R., Mikkelsen, T.S., Jacks, T., Hacohen, N., Bernstein, B.E., Kellis, M., Regev, A., Rinn, J.L., and Lander, E.S. (2009). Chromatin signature reveals over a thousand highly conserved large non-coding RNAs in mammals. Nature *458*, 223-227.

He, J., Bhat, G., Kankasa, C., Chintu, C., Mitchell, C., Duan, W., and Wood, C. (1998). Seroprevalence of human herpesvirus 8 among Zambian women of childbearing age without Kaposi's sarcoma (KS) and mother-child pairs with KS. J Infect Dis *178*, 1787-1790.

Hu, B., Huo, Y., Chen, G., Yang, L., Wu, D., and Zhou, J. (2016). Functional prediction of differentially expressed lncRNAs in HSV-1 infected human foreskin fibroblasts. Virol J *13*, 137.

Jackson, B.R., Noerenberg, M., and Whitehouse, A. (2014). A novel mechanism inducing genome instability in Kaposi's sarcoma-associated herpesvirus infected cells. PLoS Pathog *10*, e1004098.

Jham, B.C., Ma, T., Hu, J., Chaisuparat, R., Friedman, E.R., Pandolfi, P.P., Schneider, A., Sodhi, A., and Montaner, S. (2011). Amplification of the angiogenic signal through the activation of the TSC/mTOR/HIF axis by the KSHV vGPCR in Kaposi's sarcoma. PLoS One *6*, e19103.

Jiang, M., Zhang, S., Yang, Z., Lin, H., Zhu, J., Liu, L., Wang, W., Liu, S., Liu, W., Ma, Y., Zhang, L., and Cao, X. (2018). Self-Recognition of an Inducible Host lncRNA by RIG-I Feedback Restricts Innate Immune Response. Cell *173*, 906-919 e913.

Jinek, M., Chylinski, K., Fonfara, I., Hauer, M., Doudna, J.A., and Charpentier, E. (2012). A programmable dual-RNA-guided DNA endonuclease in adaptive bacterial immunity. Science *337*, 816-821.

Karcher, D.S., and Alkan, S. (1995). Herpes-like DNA sequences, AIDS-related tumors, and Castleman's disease. N Engl J Med *333*, 797-798; author reply 798-799.

Kedes, D.H., Operskalski, E., Busch, M., Kohn, R., Flood, J., and Ganem, D. (1996). The seroepidemiology of human herpesvirus 8 (Kaposi's sarcoma-associated herpesvirus): distribution of infection in KS risk groups and evidence for sexual transmission. Nat Med *2*, 918-924.

King, C.A. (2013). Kaposi's sarcoma-associated herpesvirus kaposin B induces unique monophosphorylation of STAT3 at serine 727 and MK2-mediated inactivation of the STAT3 transcriptional repressor TRIM28. J Virol *87*, 8779-8791.

Latos, P.A., Pauler, F.M., Koerner, M.V., Senergin, H.B., Hudson, Q.J., Stocsits, R.R., Allhoff, W., Stricker, S.H., Klement, R.M., Warczok, K.E., Aumayr, K., Pasierbek, P., and Barlow, D.P. (2012). Airn transcriptional overlap, but not its lncRNA products, induces imprinted Igf2r silencing. Science *338*, 1469-1472.

Li, Z., Chao, T.C., Chang, K.Y., Lin, N., Patil, V.S., Shimizu, C., Head, S.R., Burns, J.C., and Rana, T.M. (2014). The long non-coding RNA THRIL regulates TNFalpha expression through its interaction with hnRNPL. Proc Natl Acad Sci U S A *111*, 1002-1007.

Liao, W., Tang, Y., Lin, S.F., Kung, H.J., and Giam, C.Z. (2003). K-bZIP of Kaposi's sarcoma-associated herpesvirus/human herpesvirus 8 (KSHV/HHV-8) binds KSHV/HHV-8 Rta and represses Rta-mediated transactivation. J Virol *77*, 3809-3815.

Liepelt, A., Mossanen, J.C., Denecke, B., Heymann, F., De Santis, R., Tacke, F., Marx, G., Ostareck, D.H., and Ostareck-Lederer, A. (2014). Translation control of TAK1 mRNA by hnRNP K modulates LPS-induced macrophage activation. RNA *20*, 899-911.

Lin, D., Pestova, T.V., Hellen, C.U., and Tiedge, H. (2008). Translational control by a small RNA: dendritic BC1 RNA targets the eukaryotic initiation factor 4A helicase mechanism. Mol Cell Biol *28*, 3008-3019.

Lukac, D.M., Garibyan, L., Kirshner, J.R., Palmeri, D., and Ganem, D. (2001). DNA binding by Kaposi's sarcoma-associated herpesvirus lytic switch protein is necessary for transcriptional activation of two viral delayed early promoters. J Virol *75*, 6786-6799.

Ma, L., Bajic, V.B., and Zhang, Z. (2013). On the classification of long non-coding RNAs. RNA Biol *10*, 925-933.

Majerciak, V., Yamanegi, K., Allemand, E., Kruhlak, M., Krainer, A.R., and Zheng, Z.M. (2008). Kaposi's sarcoma-associated herpesvirus ORF57 functions as a viral splicing factor and promotes expression of intron-containing viral lytic genes in spliceosome-mediated RNA splicing. J Virol *82*, 2792-2801.

Malik, P., and Clements, J.B. (2004). Protein kinase CK2 phosphorylation regulates the interaction of Kaposi's sarcoma-associated herpesvirus regulatory protein ORF57 with its multifunctional partner hnRNP K. Nucleic Acids Res *32*, 5553-5569.

Massimelli, M.J., Kang, J.G., Majerciak, V., Le, S.Y., Liewehr, D.J., Steinberg, S.M., and Zheng, Z.M. (2011). Stability of a long non-coding viral RNA depends on a 9-nt core element at the RNA 5' end to interact with viral ORF57 and cellular PABPC1. Int J Biol Sci *7*, 1145-1160.

Mesri, E.A., Cesarman, E., and Boshoff, C. (2010). Kaposi's sarcoma and its associated herpesvirus. Nat Rev Cancer *10*, 707-719.

Moumen, A., Masterson, P., O'Connor, M.J., and Jackson, S.P. (2005). hnRNP K: an HDM2 target and transcriptional coactivator of p53 in response to DNA damage. Cell *123*, 1065-1078.

Myoung, J., and Ganem, D. (2011). Generation of a doxycycline-inducible KSHV producer cell line of endothelial origin: maintenance of tight latency with efficient reactivation upon induction. J Virol Methods *174*, 12-21.

Nguyen, V.T., Kiss, T., Michels, A.A., and Bensaude, O. (2001). 7SK small nuclear RNA binds to and inhibits the activity of CDK9/cyclin T complexes. Nature *414*, 322-325.

Nishitsuji, H., Ujino, S., Yoshio, S., Sugiyama, M., Mizokami, M., Kanto, T., and Shimotohno, K. (2016). Long non-coding RNA #32 contributes to antiviral responses by controlling interferon-stimulated gene expression. Proc Natl Acad Sci U S A *113*, 10388-10393.

Park, M.K., Cho, H., Roh, S.W., Kim, S.J., and Myoung, J. (2019). Cell Type-Specific Interferon-gamma-mediated Antagonism of KSHV Lytic Replication. Sci Rep *9*, 2372.

Peng, X., Gralinski, L., Armour, C.D., Ferris, M.T., Thomas, M.J., Proll, S., Bradel-Tretheway, B.G., Korth, M.J., Castle, J.C., Biery, M.C., Bouzek, H.K., Haynor, D.R., Frieman, M.B., Heise, M., Raymond,

C.K., Baric, R.S., and Katze, M.G. (2010). Unique signatures of long non-coding RNA expression in response to virus infection and altered innate immune signaling. mBio *1*.

Pringle, E.S., Robinson, C.A., and McCormick, C. (2019). Kaposi's Sarcoma-Associated Herpesvirus Lytic Replication Interferes with mTORC1 Regulation of Autophagy and Viral Protein Synthesis. J Virol *93*.

Purushothaman, P., Uppal, T., and Verma, S.C. (2015). Molecular biology of KSHV lytic reactivation. Viruses *7*, 116-153.

Rion, N., & Rüegg, M. A. (2017). LncRNA-encoded peptides: More than translational noise?. Cell research *27*, 604–605.

Rossetto, C.C., and Pari, G. (2012). KSHV PAN RNA associates with demethylases UTX and JMJD3 to activate lytic replication through a physical interaction with the virus genome. PLoS Pathog *8*, e1002680.

Rossetto, C.C., Tarrant-Elorza, M., Verma, S., Purushothaman, P., and Pari, G.S. (2013). Regulation of viral and cellular gene expression by Kaposi's sarcoma-associated herpesvirus polyadenylated nuclear RNA. J Virol *87*, 5540-5553.

Sakakibara, S., and Tosato, G. (2011). Viral interleukin-6: role in Kaposi's sarcoma-associated herpesvirus: associated malignancies. J Interferon Cytokine Res *31*, 791-801.

Schulz, T.F. (2000). Kaposi's sarcoma-associated herpesvirus (human herpesvirus 8): epidemiology and pathogenesis. J Antimicrob Chemother *45 Suppl T3*, 15-27.

Si, H., and Robertson, E.S. (2006). Kaposi's sarcoma-associated herpesvirus-encoded latency-associated nuclear antigen induces chromosomal instability through inhibition of p53 function. J Virol *80*, 697-709.

Song, M.J., Li, X., Brown, H.J., and Sun, R. (2002). Characterization of interactions between RTA and the promoter of polyadenylated nuclear RNA in Kaposi's sarcoma-associated herpesvirus/human herpesvirus 8. J Virol *76*, 5000-5013.

Sturzl, M., Gaus, D., Dirks, W.G., Ganem, D., and Jochmann, R. (2013). Kaposi's sarcoma-derived cell line SLK is not of endothelial origin, but is a contaminant from a known renal carcinoma cell line. Int J Cancer *132*, 1954-1958.

Sun, R., Lin, S.F., Staskus, K., Gradoville, L., Grogan, E., Haase, A., and Miller, G. (1999). Kinetics of Kaposi's sarcoma-associated herpesvirus gene expression. J Virol *73*, 2232-2242.

Tan, B., Liu, H., Zhang, S., da Silva, S.R., Zhang, L., Meng, J., Cui, X., Yuan, H., Sorel, O., Zhang, S.W., Huang, Y., and Gao, S.J. (2018). Viral and cellular N(6)-methyladenosine and N(6),2'-O-dimethyladenosine epitranscriptomes in the KSHV life cycle. Nat Microbiol *3*, 108-120.

Tomlinson, C.C., and Damania, B. (2004). The K1 protein of Kaposi's sarcoma-associated herpesvirus activates the Akt signaling pathway. J Virol *78*, 1918-1927.

Toth, Z., Brulois, K., and Jung, J.U. (2013). The chromatin landscape of Kaposi's sarcoma-associated herpesvirus. Viruses *5*, 1346-1373.

Tripathi, V., Ellis, J.D., Shen, Z., Song, D.Y., Pan, Q., Watt, A.T., Freier, S.M., Bennett, C.F., Sharma, A., Bubulya, P.A., Blencowe, B.J., Prasanth, S.G., and Prasanth, K.V. (2010). The nuclear-retained non-coding RNA MALAT1 regulates alternative splicing by modulating SR splicing factor phosphorylation. Mol Cell *39*, 925-938.

Tsai, P.L., Chiou, N.T., Kuss, S., Garcia-Sastre, A., Lynch, K.W., and Fontoura, B.M. (2013). Cellular RNA binding proteins NS1-BP and hnRNP K regulate influenza A virus RNA splicing. PLoS Pathog *9*, e1003460.

Ulitsky, I., and Bartel, D.P. (2013). lincRNAs: genomics, evolution, and mechanisms. Cell *154*, 26-46.

Wang, S.E., Wu, F.Y., Fujimuro, M., Zong, J., Hayward, S.D., and Hayward, G.S. (2003a). Role of CCAAT/enhancer-binding protein alpha (C/EBPalpha) in activation of the Kaposi's sarcoma-associated herpesvirus (KSHV) lytic-cycle replication-associated protein (RAP) promoter in cooperation with the KSHV replication and transcription activator (RTA) and RAP. J Virol *77*, 600-623.

Wang, S.E., Wu, F.Y., Yu, Y., and Hayward, G.S. (2003b). CCAAT/enhancer-binding protein-alpha is induced during the early stages of Kaposi's sarcoma-associated herpesvirus (KSHV) lytic cycle reactivation and together with the KSHV replication and transcription activator (RTA) cooperatively stimulates the viral RTA, MTA, and PAN promoters. J Virol *77*, 9590-9612.

Wang, Y., Li, H., Tang, Q., Maul, G.G., and Yuan, Y. (2008). Kaposi's sarcoma-associated herpesvirus ori-Lyt-dependent DNA replication: involvement of host cellular factors. J Virol *82*, 2867-2882.

Wu, T.H., Shi, L., Lowe, A.W., Nicolls, M.R., and Kao, P.N. (2019). Inducible expression of immediate early genes is regulated through dynamic chromatin association by NF45/ILF2 and NF90/NF110/ILF3. PLoS One *14*, e0216042.

Xie, Q., Chen, S., Tian, R., Huang, X., Deng, R., Xue, B., Qin, Y., Xu, Y., Wang, J., Guo, M., Chen, J., Tang, S., Li, G., and Zhu, H. (2018). Long Non-coding RNA ITPRIP-1 Positively Regulates the Innate Immune Response through Promotion of Oligomerization and Activation of MDA5. J Virol *92*.

Yarchoan, R., Tosato, G., and Little, R.F. (2005). Therapy insight: AIDS-related malignancies--the influence of antiviral therapy on pathogenesis and management. Nat Clin Pract Oncol *2*, 406-415; quiz 423.

Yu, F., Harada, J.N., Brown, H.J., Deng, H., Song, M.J., Wu, T.T., Kato-Stankiewicz, J., Nelson, C.G., Vieira, J., Tamanoi, F., Chanda, S.K., and Sun, R. (2007). Systematic identification of cellular signals reactivating Kaposi sarcoma-associated herpesvirus. PLoS Pathog *3*, e44.

Zhang, H., Ni, G., and Damania, B. (2020). ADAR1 Facilitates KSHV Lytic Reactivation by Modulating the RLR-Dependent Signaling Pathway. Cell Rep *31*, 107564.

Zhang, Q., Chao, T.C., Patil, V.S., Qin, Y., Tiwari, S.K., Chiou, J., Dobin, A., Tsai, C.M., Li, Z., Dang, J., Gupta, S., Urdahl, K., Nizet, V., Gingeras, T.R., Gaulton, K.J., and Rana, T.M. (2019). The long non-coding RNA ROCKI regulates inflammatory gene expression. EMBO J *38*.

Zhang, Q., Lai, M.M., Lou, Y.Y., Guo, B.H., Wang, H.Y., and Zheng, X.Q. (2016). Transcriptome altered by latent human cytomegalovirus infection on THP-1 cells using RNA-seq. Gene *594*, 144-150.

Zhong, W., Wang, H., Herndier, B., and Ganem, D. (1996). Restricted expression of Kaposi sarcoma-associated herpesvirus (human herpesvirus 8) genes in Kaposi sarcoma. Proc Natl Acad Sci U S A *93*, 6641-6646.